UC Riverside

UC Riverside Previously Published Works

Title

Seizure-induced alterations in fast-spiking basket cell GABA currents modulate frequency and coherence of gamma oscillation in network simulations

Permalink

https://escholarship.org/uc/item/5xf6c1tw

Journal

Chaos An Interdisciplinary Journal of Nonlinear Science, 23(4)

ISSN

1054-1500

Authors

Proddutur, Archana
Yu, Jiandong
Elgammal, Fatima S
et al.

Publication Date

2013-12-01

DOI

10.1063/1.4830138

Peer reviewed

eScholarship.org Powered by the California Digital Library
University of California

Seizure-induced alterations in fast-spiking basket cell GABA currents modulate frequency and coherence of gamma oscillation in network simulations

Archana Proddutur,[1] Jiandong Yu,[1] Fatima S. Elgammal,[1]
and Vijayalakshmi Santhakumar[1,2,a)]
[1]*Department of Neurology and Neurosciences, New Jersey Medical School, Rutgers, Newark, New Jersey 07103, USA*
[2]*Department of Pharmacology and Physiology, New Jersey Medical School, Rutgers, Newark, New Jersey 07103, USA*

(Received 10 April 2013; accepted 30 October 2013; published online 20 November 2013)

Gamma frequency oscillations have been proposed to contribute to memory formation and retrieval. Fast-spiking basket cells (FS-BCs) are known to underlie development of gamma oscillations. Fast, high amplitude GABA synapses and gap junctions have been suggested to contribute to gamma oscillations in FS-BC networks. Recently, we identified that, apart from GABAergic synapses, FS-BCs in the hippocampal dentate gyrus have GABAergic currents mediated by extrasynaptic receptors. Our experimental studies demonstrated two specific changes in FS-BC GABA currents following experimental seizures [Yu *et al.*, J. Neurophysiol. **109**, 1746 (2013)]: increase in the magnitude of extrasynaptic (tonic) GABA currents and a depolarizing shift in GABA reversal potential (E_{GABA}). Here, we use homogeneous networks of a biophysically based model of FS-BCs to examine how the presence of extrasynaptic GABA conductance ($g_{GABA\text{-}extra}$) and experimentally identified, seizure-induced changes in $g_{GABA\text{-}extra}$ and E_{GABA} influence network activity. Networks of FS-BCs interconnected by fast GABAergic synapses developed synchronous firing in the dentate gamma frequency range (40–100 Hz). Systematic investigation revealed that the biologically realistic range of 30 to 40 connections between FS-BCs resulted in greater coherence in the gamma frequency range when networks were activated by Poisson-distributed dendritic synaptic inputs rather than by homogeneous somatic current injections, which were balanced for FS-BC firing frequency in unconnected networks. Distance-dependent conduction delay enhanced coherence in networks with 30–40 FS-BC interconnections while inclusion of gap junctional conductance had a modest effect on coherence. In networks activated by somatic current injections resulting in heterogeneous FS-BC firing, increasing $g_{GABA\text{-}extra}$ reduced the frequency and coherence of FS-BC firing when E_{GABA} was shunting (−74 mV), but failed to alter average FS-BC frequency when E_{GABA} was depolarizing (−54 mV). When FS-BCs were activated by biologically based dendritic synaptic inputs, enhancing $g_{GABA\text{-}extra}$ reduced the frequency and coherence of FS-BC firing when E_{GABA} was shunting and increased average FS-BC firing when E_{GABA} was depolarizing. Shifting E_{GABA} from shunting to depolarizing potentials consistently increased network frequency to and above high gamma frequencies (>80 Hz). Since gamma oscillations may contribute to learning and memory processing [Fell *et al.*, Nat. Neurosci. **4**, 1259 (2001); Jutras *et al.*, J. Neurosci. **29**, 12521 (2009); Wang, Physiol. Rev. **90**, 1195 (2010)], our demonstration that network oscillations are modulated by extrasynaptic inhibition in FS-BCs suggests that neuroactive compounds that act on extrasynaptic GABA receptors could impact memory formation by modulating hippocampal gamma oscillations. The simulation results indicate that the depolarized FS-BC GABA reversal, observed after experimental seizures, together with enhanced spillover extrasynaptic GABA currents are likely to promote generation of focal high frequency activity associated with epileptic networks. © *2013 AIP Publishing LLC*.
[http://dx.doi.org/10.1063/1.4830138]

Among the rhythmic firing patterns observed in brain networks, gamma oscillations are generated by a specific class of inhibitory neurons with robust interconnectivity through fast GABA synapses. Recently, we identified the presence of a tonic, slow form of GABA currents in these neurons and showed that experimentally induced seizures increase the magnitude of tonic GABA currents and render GABA currents depolarizing. By simulating networks composed of biophysically based models of the specific inhibitory neuron involved in gamma oscillations, we show that the presence of the tonic GABA currents can influence the robustness of gamma oscillations. Since tonic GABA currents are known to be altered by neuroactive compounds, such as alcohol, steroids, and anesthetics, our findings suggest a mechanism by which these agents may impact network oscillations. Moreover, we find that the experimentally detected, seizure-induced

a)Author to whom correspondence should be addressed. E-mail: santhavi@njms.rutgers.edu

 © 2013 AIP Publishing LLC

changes in GABA currents promote network activity at abnormally high frequencies observed in epilepsy.

INTRODUCTION

Brain networks are characterized by the presence of oscillatory activity over a wide range of frequencies from the slow delta waves (0.5–3 Hz) to high frequency oscillations such as ripples (140–200 Hz) (Buzsaki *et al.*, 2003; Buzsaki and Draguhn, 2004). Among the brain oscillations, the gamma frequency oscillations (30–140 Hz), which are present in several brain regions (Steriade *et al.*, 1996; Csicsvari *et al.*, 1999; Csicsvari *et al.*, 2003; Colgin and Moser, 2010; Wang, 2010; Buzsaki and Wang, 2012), including hippocampal circuits, have been extensively investigated because of their proposed role as a reference signal in temporal encoding, contributions to binding of sensory feature, and their role in memory formation and retrieval (Lisman and Idiart, 1995; Fell *et al.*, 2001; Bartos *et al.*, 2007; Montgomery and Buzsaki, 2007; Jutras *et al.*, 2009). Studies vary in the exact frequency range denoted as gamma oscillations (Csicsvari *et al.*, 2003; Bragin *et al.*, 2005; Colgin and Moser, 2010; Buzsaki and Wang, 2012). In the hippocampal CA1, gamma frequency oscillations have been shown to occur at two frequency ranges: slow gamma (~30–50 Hz) driven by CA3, and fast (65–140 Hz) gamma driven by entorhinal inputs (Csicsvari *et al.*, 1999; Colgin *et al.*, 2009; Colgin and Moser, 2010), although recent studies suggest that fast gamma may be composed of two mechanistically distinct frequencies (Belluscio *et al.*, 2012; Buzsaki and Wang, 2012). In the dentate gyrus, which has the largest gamma amplitude in the hippocampus, gamma frequency oscillations are reported to be in the 40–100 Hz range (Bragin *et al.*, 1995). Inputs from the entorhinal cortex are crucial in maintaining high gamma frequency oscillations in the dentate gyrus (Bragin *et al.*, 1995). A large body of experimental and theoretical work suggests that rhythmic activity of synaptically interconnected inhibitory neurons contribute to generation of hippocampal gamma oscillations (Wang and Buzsaki, 1996; Traub *et al.*, 1998; Whittington *et al.*, 2000; Bartos *et al.*, 2002; Brunel and Wang, 2003), although additional mechanisms likely contribute to gamma oscillations *in vivo* (Wulff *et al.*, 2009). Indeed, hippocampal gamma oscillations, including those induced by agonists of metabotropic glutamate and muscarinic acetylcholine receptors *in vitro*, can be completely blocked by $GABA_A$ receptor ($GABA_AR$) antagonists, further indicating the critical role for inhibition in generation of gamma oscillations (Whittington *et al.*, 1995; Fisahn *et al.*, 1998; Mann *et al.*, 2005). Among the diverse classes of inhibitory interneurons, the fast-spiking basket cells (FS-BCs) that express the calcium binding protein parvalbumin appear to be essential for the generation of gamma oscillations in the dentate gyrus (Bartos *et al.*, 2007). Parvalbumin-positive basket cells are characterized by high mutual interconnectivity through fast synaptic inhibition and electrical coupling (Fukuda and Kosaka, 2000; Bartos *et al.*, 2002; Galarreta and Hestrin, 2002; Hefft and Jonas, 2005). Additionally, parvalbumin basket cells have high intrinsic firing, low adaptation, and an intrinsic resonance frequency, which make them an optimal candidate to fire in phase with gamma frequency oscillations (Pike *et al.*, 2000; Hefft and Jonas, 2005). FS-BCs innervate a large population of excitatory neurons, which they can synchronize. Modeling studies have provided compelling evidence that homogeneous networks composed of fast-spiking neurons randomly interconnected by synaptic inhibition can generate gamma frequency oscillations when activated by excitatory current injections (Wang and Buzsaki, 1996). Subsequently, studies in networks of generic single compartment models of fast-spiking neurons connected to a biologically based number of local neighbors have demonstrated that incorporating the experimentally determined rapid synaptic decay kinetics between FS-BCs leads the network to synchronize in the gamma frequency range, even in networks activated by heterogeneous current injections (Bartos *et al.*, 2002). Since network responses are strongly regulated by intrinsic neuronal properties (Tateno *et al.*, 2004; Tateno and Robinson, 2006; Borgers and Walker, 2013), whether conclusions derived using generic models are robust to inclusion of biophysically based model parameters remains to be examined.

One of the salient findings in simulation studies using homogeneous, synaptically connected inhibitory networks is that the frequency and coherence of network oscillations are regulated by the delay and decay kinetics of the GABA synapses (Bartos *et al.*, 2002; Brunel and Wang, 2003; Bartos *et al.*, 2007). Recently, we reported that, apart from the classical synaptic GABA currents, parvalbumin-positive, FS-BCs in the dentate gyrus express extrasynaptic (tonic) GABA currents (Yu *et al.*, 2013). Extrasynaptic GABA currents are mediated by extra- and peri-synaptically located $GABA_AR$s and can contribute to the decay kinetics of synaptic GABA receptors (Wei *et al.*, 2003; Santhakumar *et al.*, 2006; Glykys and Mody, 2007). Spillover of GABA from the synapse can activate extrasynaptic $GABA_AR$s and lead to prolonged GABAergic inhibition (Wei *et al.*, 2003; Santhakumar *et al.*, 2006) and slow spillover synaptic currents (Rossi and Hamann, 1998). Since the decay kinetics of synaptic inhibition regulate gamma oscillations (Bartos *et al.*, 2002), extrasynaptic GABA currents in FS-BCs are likely to modulate these rhythms. Consistent with this hypothesis, studies in hippocampal slices from mice lacking specific $GABA_AR$ subunits underlying extrasynaptic GABA currents have identified alterations in gamma rhythms (Mann and Mody, 2010). However, whether extrasynaptic GABA currents in FS-BCs modulate the coherence and frequency of network oscillation has not been examined.

Several studies have identified alterations in gamma oscillations in neurological disorders including epilepsy and schizophrenia (Hirai *et al.*, 1999; Worrell *et al.*, 2004; Bragin *et al.*, 2005; Uhlhaas and Singer, 2010; Lewis *et al.*, 2012). Our recent experimental studies have uncovered that status epilepticus in an animal model of epilepsy leads to two specific alterations in GABA currents in dentate FS-BCs. First, extrasynaptic GABA currents in FS-BCs are enhanced following pilocarpine-induced status epilepticus (Yu *et al.*, 2013). How this increase in FS-BC tonic GABA

currents may impact generation of oscillations in FS-BC networks is currently unknown. Second, we found that the reversal potential for GABA currents (E_{GABA}) in FS-BCs is significantly depolarized following experimental status epilepticus (Yu *et al.*, 2013). Curiously, apart from the kinetics of synaptic inhibition, the presence of shunting rather than hyperpolarizing reversal potential of synaptic GABA currents has also been shown to increase the frequency and reduce coherence of oscillations in homogeneous interneuronal networks (Vida *et al.*, 2006). Alterations in the frequency of network oscillations can be of clinical significance, since oscillations over a frequency of 100 Hz, in the range of high gamma and high frequency oscillations, can be associated with epileptic foci in the hippocampus and cortex (Bragin *et al.*, 2004; Worrell *et al.*, 2004; Engel *et al.*, 2009). However, it is difficult to intuit how the seizure-induced increase in FS-BC tonic GABA currents and depolarizing shift in GABA reversal potential, observed in our experimental studies (Yu *et al.*, 2013) would interact to modify FS-BC network activity. Here, we use homogeneous networks of biophysically based, multi-compartmental model FS-BCs to examine how the presence of extrasynaptic GABA currents and the experimentally identified seizure-induced alterations in GABA currents and E_{GABA} modify the frequency and coherence of network firing.

MATERIAL AND METHODS

Slice preparation and physiology

All procedures were performed under protocols approved by the University of Medicine and Dentistry of New Jersey, Newark, NJ, Institutional Animal Care and Use Committee. Young adult, male, Wistar rats between postnatal days 30–35 were anesthetized with isoflurane and decapitated. Horizontal brain slices (300 μm) were prepared in ice-cold sucrose artificial cerebrospinal fluid (CSF) (sucrose-aCSF) containing (in mM) 85 NaCl, 75 sucrose, 24 $NaHCO_3$, 25 glucose, 4 $MgCl_2$, 2.5 KCl, 1.25 NaH_2PO_4, and 0.5 $CaCl_2$, using a Leica VT1200S Vibratome (Wetzlar, Germany). The slices were incubated at 32 ± 1 °C for 30 min in a submerged holding chamber containing an equal volume of sucrose-aCSF and recording aCSF and subsequently held at room temperature (RT). The recording aCSF contained (in mM) 126 NaCl, 2.5 KCl, 2 $CaCl_2$, 2 $MgCl_2$, 1.25 NaH_2PO_4, 26 $NaHCO_3$ and 10 D-glucose. All solutions were saturated with 95% O_2 and 5% CO_2 and maintained at a pH of 7.4 for 1–6 h. Slices were transferred to a submerged recording chamber and perfused with oxygenated aCSF at 33 ± 1 °C. Whole-cell current-clamp recordings from interneurons at the border of the hilus and granule cell layer were obtained under IR-DIC visualization using microelectrodes (5–7 MΩ) containing (in mM) 125 KCl, 10 K-gluconate, 10 HEPES, 2 $MgCl_2$, 0.2 ethylene glycol tetraacetic acid, 2 Na-ATP, 0.5 Na-GTP, and 10 PO Creatine titrated to a pH 7.25 with KOH. Biocytin (0.2%) was included in the internal solution for post-hoc cell identification (Gupta *et al.*, 2012; Yu *et al.*, 2013). Recordings were obtained using Axon Instruments MultiClamp 700B (Molecular Devices, Sunnyvale, CA). Data were low-pass filtered at 3 kHz, digitized using DigiData 1440 A and acquired using pClamp10 at 10-kHz sampling frequency. Recorded neurons were held at −70 mV and the response to 1.5 s positive and negative current injections were examined to determine active and passive characteristics. Cells with non-adapting, high frequency firing for the entire duration of the current injection, and low input resistance (<150 MΩ), were classified as FS-BCs (Hefft and Jonas, 2005; Yu *et al.*, 2013). Neurons with adapting firing, high input resistance (>150 MΩ), and sag during negative current injection were excluded from analysis. Post-hoc biocytin immunostaining and morphological analysis was used to definitively identify FS-BCs, on the basis of presence of axon terminals in the granule cell layer and immunostaining for parvalbumin (Yu *et al.*, 2013). Following physiological recordings, slices were fixed in 0.1 M phosphate buffer containing 4% paraformaldehyde at 4 °C for 2 days. Slices were incubated overnight at room temperature with anti-parvalbumin antibody (PV-28, 1.5:1000, polyclonal rabbit, Swant) in 0.3% Triton X-100 and 2% normal goat serum containing phosphate-buffered saline (PBS). Immunoreactions were revealed using Alexa 488-conjugated secondary goat antibodies against rabbit IgG (1:250) and biocytin staining was revealed using Alexa 594-conjugated streptavidin (1:1000). Sections were visualized and imaged using a Nikon A1R laser confocal microscope with a 0.75 NA 20X air objective (Gupta *et al.*, 2012; Yu *et al.*, 2013).

Basket cell simulations

Individual FS-BC models and FS-BC network simulations were implemented using the NEURON 7.0 simulation environment (Hines and Carnevale, 1997). The biophysically based FS-BC model was adapted from earlier studies (Santhakumar *et al.*, 2005; Dyhrfjeld-Johnsen *et al.*, 2007). The model FS-BC included a soma with 2 apical and 2 basal dendrites each with 4 distinct proximal (1°) to distal (4°) compartments (Fig. 1(b)). Active and passive conductances were distributed as detailed previously (Santhakumar *et al.*, 2005). Sodium and fast-delayed rectifier potassium channels were restricted to the soma and proximal (1°) dendritic compartments. Other active conductances including A-Type potassium channels, L and N-Type calcium channels, Ca-dependent potassium (SK) channels, and Ca and voltage-dependent potassium (BK) channels were distributed uniformly in all compartments as detailed previously (Santhakumar *et al.*, 2005). A non-specific leak conductance with reversal potential set to −75 mV and conductance set to 0.14 mS/cm^2 in the soma and 0.12 mS/cm^2 in all dendritic compartments was included to model the experimentally observed input resistance (Yu *et al.*, 2013). Gap junctions were implemented as an intercellular conductance (Bartos *et al.*, 2002) located randomly in all four (1° to 4°) dendritic compartments. In an initial set of experiments (Fig. 2) designed to determine the effect of gap junctional conductance on cellular input resistance, total gap junctional conductance to the model FS-BC was systematically varied between 1 and 10^6 pS. Input resistance was measured in response to a −100 pA somatic current injection. Baseline extrasynaptic GABA conductance was modeled as a linear

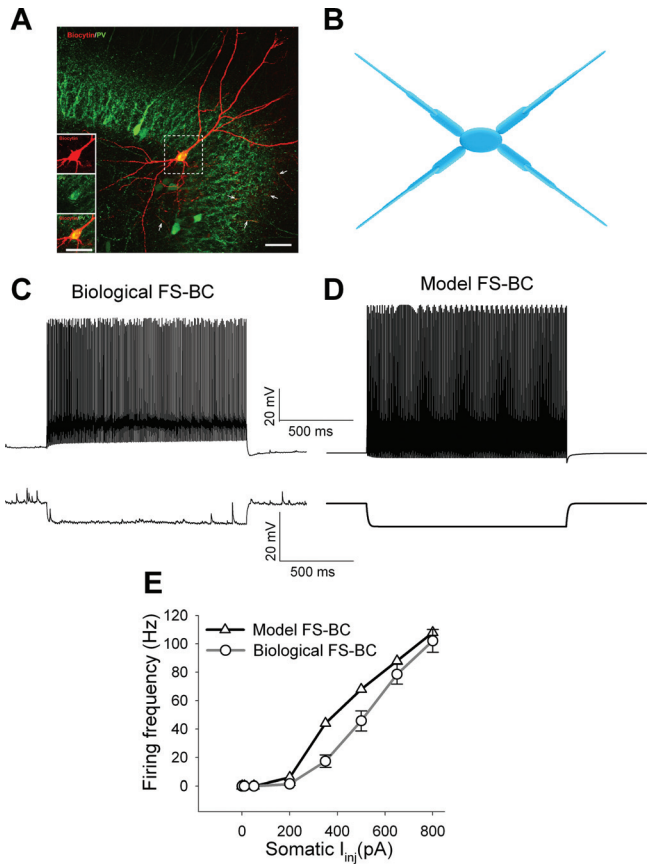

FIG. 1. Structure and intrinsic properties of model fast-spiking basket cell. (a) Projection of confocal image stacks of a fast-spiking basket cell (FS-BC) filled with biocytin (red) during recordings and labeled for parvalbumin (PV, green) shows the typical morphology with and axon in granule cell layer (arrows). *Insets:* Confocal image of biocytin-filled soma (top in red) and labeling for PV (middle in green). Merged image (bottom) shows PV and biocytin co-labeling in the soma. Scale bar, 50 μm. (b) Schematic representation of the structure of the model FS-BC. (c) and (d) Membrane voltage traces from the biological (c) and model FS-BC (d) illustrates the fast-spiking, non-adapting firing pattern during a +500 pA current injection and relatively low membrane hyperpolarization in response to a −50 pA current injection. (e) Overlay of the firing rates of biological and model FS-BCs in response to increasing current injections.

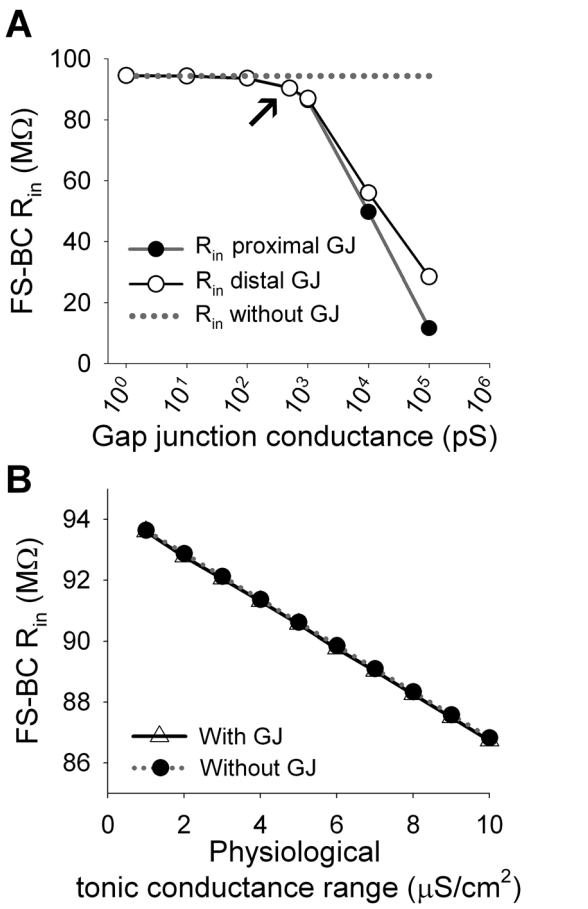

FIG. 2. Effect of gap junctions and extrasynaptic GABA conductance on model FS-BC input resistance of cell. (a) Plot shows the input resistance of a model FS-BC in the presence of progressively increasing the gap junctional conductance between a FS-BC pair. Input resistance at the gap junctional conductance used in network simulations is indicated by the arrow. Dotted line represents FS-BC input resistance in the absence of gap junctions. (b) Plot shows FS-BC input resistance when the baseline extrasynaptic GABA conductance was increased in the physiologically relevant range. FS-BC pairs were simulated with and without 500 pS gap junctional conductance.

deterministic leak conductance with the GABA reversal potential (E_{GABA}) set to −74 mV, the experimentally determined value in FS-BCs under control conditions (Song *et al.*, 2011; Yu *et al.*, 2013). Extrasynaptic GABA conductance ($g_{GABA\text{-}extra}$) was distributed uniformly in the somatic and all dendritic compartments and varied between 2 and 10 μS/cm^2. This conductance range was set to replicate the biologically relevant extrasynaptic GABA current range of 10 to 60 pA in model FS-BCs under voltage clamp conditions, as detailed earlier (Yu *et al.*, 2013). The biologically relevant extrasynaptic GABA current range of 10 to 60 pA was derived based on experimental measurements during whole cell patch clamp recordings in dentate FS-BCs (Yu *et al.*, 2013).

Network simulations

Structurally realistic FS-BC network models were simulated with 200 FS-BCs arranged on a virtual ring with 50 μm spacing between adjacent cells (Bartos *et al.*, 2002; Vida *et al.*, 2006). FS-BCs were connected by $GABA_A$ synapses located on the proximal (1°) apical dendrite as described previously (Santhakumar *et al.*, 2005). Exp2Syn process in NEURON was used to implement chemical synapses. Based on data from experimental studies, $GABA_A$ synapses between FS-BCs were simulated with a maximum synaptic conductance of 7.6 ns, rise and decay time constants of 0.16 and 1.8 ms, respectively, and a 0.8 ms synaptic delay (Bartos *et al.*, 2002; Santhakumar *et al.*, 2005). In an initial set of simulations, the number of synaptic connections between FS-BCs was systematically increased from 4 to 100 connections distributed uniformly among neighboring FS-BCs on either side. While all $GABA_A$ synapses included a synaptic delay of 0.8 ms, in some simulations, an additional distance-dependent "conduction delay" was included. The conduction delay was calculated from the distance between pre- and postsynaptic cell along the circumference of the ring and an estimated conduction velocity of 0.25 m/s (Bartos *et al.*, 2002). In a subset of simulations, each neuron was connected to 50 nearest neighbors by electrical synapses distributed among all four dendritic compartments. Distribution of gap junctions in the dendrites and exclusion

from the somatic compartments was based on experimental data (Amitai *et al.*, 2002). Consistent with experimental data on the single channel conductance of connexin 36 channels (Srinivas *et al.*, 1999), conductance of a single electrical synapse was set to 10 pS.

Experimental studies have shown that synaptic GABA release during neuronal activity can increase extrasynaptic GABA levels and contribute to transient enhancement of baseline tonic GABA currents (Glykys and Mody, 2007). In the dentate gyrus, $GABA_A$ receptor δ subunits underlie tonic GABA currents are located perisynaptically, and can be readily activated by spillover of GABA from the synapse and thereby contribute to prolongation of synaptic decay (Wei *et al.*, 2003). Consistent with the prediction that synaptic spillover augments tonic GABA currents (Glykys and Mody, 2007), network simulations with extrasynaptic GABA currents included both baseline and "spillover" $g_{GABA\text{-}extra}$. Spillover inhibition was modeled by assuming 2 concentric circles around each synapse and introducing "spillover" $g_{GABA\text{-}extra}$ with slower rise (7 ms) and decay time constants (200 ms) than the corresponding synaptic processes as detailed previously (Yu *et al.*, 2013). Due to the lack of experimental data on the kinetics of spillover GABA currents in dentate FS-BCs, the slow rise and decay time for spillover GABA currents were assumed based on experimental data conducted in the cerebellum at room temperature showing that presumed spillover spontaneous inhibitory postsynaptic currents have a rise times of over 10 ms and decay times of over 200 ms (Rossi and Hamann, 1998). When "baseline" tonic GABA was set to 2 μS, to simulate the tonic GABA current levels measured from FS-BCs in control rats not subject to pilocarpine- induced status epilepticus (Yu *et al.*, 2013), peak conductance of the spillover $g_{GABA\text{-}extra}$ were set to 1.25 pS for the first spillover synapse and 0.125 pS for the second spillover synapse to simulate the reduction in GABA levels as one moved away from the primary synapse. In simulations examining the effect of increasing tonic GABA currents, the peak conductance of the spillover $g_{GABA\text{-}extra}$ was correspondingly increased by a factor reflecting the degree of enhancement of baseline extrasynaptic GABA currents (ratio of baseline $g_{GABA\text{-}extra}$ in a given simulation in $\mu S/cm^2$ to baseline $g_{GABA\text{-}extra}$ of 2 $\mu S/cm^2$) as detailed previously (Yu *et al.*, 2013). For example when baseline $g_{GABA\text{-}extra}$ was 4 and 6 μS, two and three times the control level of 2 μS, the peak $g_{GABA\text{-}extra}$ of the first spillover synapse was set to 2.5 pS and 3.75 pS, respectively. Similarly, since spillover spread would occur over an area, the second spillover synapse was set to 0.5 pS (2^2*0.125 pS) and 1.125 (3^2*0.125 pS), respectively.

Networks were activated either by somatic current injections or by excitatory dendritic synaptic inputs. In simulations where the network response to dendritic synaptic inputs and somatic current injections were compared (Fig. 3), the somatic current injection was set to 600 pA, so that both dendritic synaptic inputs and somatic current injections result in similar average FS-BC frequency in an unconnected network, defined as a network without inhibitory synapses or gap junctions. In networks activated by somatic current injections, the mean somatic current injection was systematically varied between 300 and 700 pA. Heterogeneity in

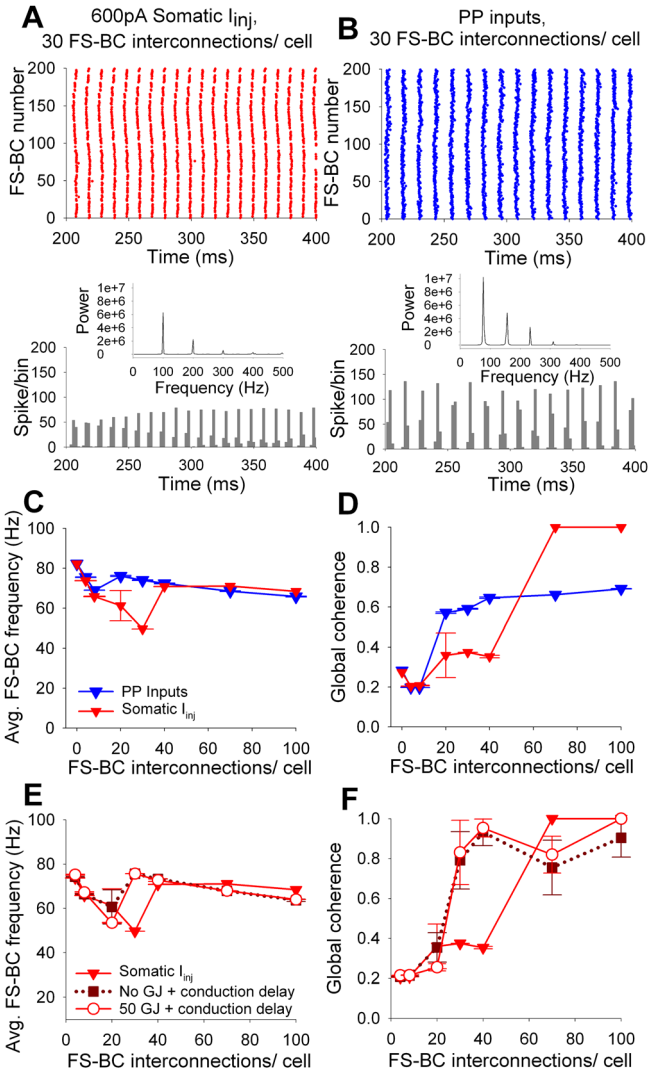

FIG. 3. Impact of FS-BC synaptic interconnectivity on frequency and coherence of network firing. (a) and (b) Representative spike rasters (top panels) of networks with 30 FS-BC interconnections/cell showing network activity when stimulated by a 600 pA homogeneous somatic current injection (somatic I_{inj} in red, (a)) and dendritic synaptic inputs modeled after perforant path synapses (PP Inputs in blue, (b)). Corresponding spike-time histograms (bottom panels) show the coherent activity in (a) and (b). Insets in bottom panels of (a) and (b) show corresponding frequency power plots. (c) and (d) Effect of progressively increasing interneuronal interconnectivity on average FS-BC frequency (c) and coherence (d) in networks activated by somatic I_{inj} in red and PP Inputs in blue. Legend in (c) applies to (c) and (d). (e) and (f). Data from networks activated by somatic current injections show the effect of including distance dependent axonal conduction delay and gap junctions (GJ) on the average FS-BC frequency (e) and coherence (f). Legend in (e) applies to (e) and (f). Data are presented as mean ± s.e.m of 3 independent runs.

FS-BC firing frequency of over 10% was generated by introducing variability in the somatic current injection to each model FS-BC in the network. The magnitude of the somatic current injection in each FS-BC was varied by randomly selecting the peak amplitude from a Gaussian distribution of amplitudes with mean peak amplitude set between 300 and 700 pA (in 100 pA steps), and either 0.1% or 0.5% heterogeneity (% heterogeneity was defined as variance/mean*100). Additionally, the time of commencement of the somatic current injection was staggered over a 70 ms time window (−20 to 50 ms of simulation time). Somatic current injections with

0.1% heterogeneity yielded 34.3% and 10.8% heterogeneity in FS-BC firing frequency in unconnected networks when the mean current injections were 300 pA and 700 pA, respectively. Similarly, mean somatic current injections of 300 pA and 700 pA at 0.5% heterogeneity resulted in 186.4% and 54.6% heterogeneity, respectively, in FS-BC firing in the unconnected network. Given the low input resistance of biologically based FS-BCs, when the heterogeneity of somatic current injections was increased to and beyond 0.5%, a considerable number of FS-BCs received somatic current injections less than the firing threshold and failed to fire even once throughout the entire period of the simulations. When E_{GABA} was −74 mV, heterogeneity of 0.5% rendered over 12% and 50% of FS-BCs completely inactive when the mean somatic current injection was 700 and 300 pA, respectively. Therefore, heterogeneities over 0.5%, which would lead to inactivation of over 50% of FS-BCs within the range of somatic current injections under study, were not examined.

In networks activated by synaptic inputs, each model FS-BC received an independent Poisson-distributed train of excitatory synaptic inputs at 200 Hz. Excitatory synapses were located in the distal (4°) dendritic compartment of the apical dendrites (Santhakumar *et al.*, 2005). The peak AMPA synaptic conductance was 20 ns and kinetics were similar to those used in previous studies (Santhakumar *et al.*, 2005; Yu *et al.*, 2013). The effects of increasing $g_{GABA\text{-}extra}$ on the average frequency and coherence of firing of FS-BCs in the mutually connected networks were examined. Unless otherwise stated, E_{GABA} of synaptic and extrasynaptic GABA currents was set to −74 mV to simulate the experimentally determined GABA reversal in FS-BCs from control rats not subject to status epilepticus (Yu *et al.*, 2013). In simulations examining how seizure-induced changes in GABA reversal impact FS-BC network activity, the reversal potential of both synaptic and extrasynaptic GABA currents was set to −54 mV to simulate the depolarized GABA reversal observed in FS-BCs after experimental status epilepticus (Yu *et al.*, 2013).

Analysis

Average FS-BC frequency was quantified as the average of the reciprocal of inter-spike intervals during 200–500 ms of the simulation after establishment of stable network firing patterns. Spike-time histograms were developed with bin width of 1 ms and used to generate corresponding frequency power spectra. Network frequency was defined as the frequency at the strongest peak power. Throughout the rest of the manuscript, we will refer to frequency calculated based on individual cell inter-spike intervals as "average FS-BC frequency" and the frequency determined from the spike-time histogram as "network frequency." Two measures were used to quantify population coherence during 200–500 ms of the simulation time. In the Wang-Buzsaki method, action potential patterns were represented in a binary format (with 0 when no action potential occurred and 1 if action potentials were generated in a given time interval). To account for differences in firing frequency, the time interval for the calculation of coherence was set to $0.2/f$, where f is the average FS-BC frequency in Hz (White *et al.*, 1998; Santhakumar *et al.*, 2005). A subset of networks activated by somatic currents injections, particularly those with 0.5% heterogeneity in current injections, resulted in a few FS-BCs that failed to fire action potentials. The inactive was excluded from the coherence analysis. Cells that failed to fire were not excluded from analysis of average FS-BC frequency. A cross-correlation-based population coherence measure was calculated as described (Wang and Buzsaki, 1996; Bartos *et al.*, 2002) using MATLAB R2012a. In the second method (White *et al.*, 1998; Santhakumar *et al.*, 2005), for each pair of discharging neurons, trains of square pulses were generated for each of the cells with each pulse of height unity being centered at the spike peak and the width being 20% of the mean firing period (inter-spike interval) of the faster cell in the pair. Next, the cross-correlation was calculated at zero time lag of these pulse trains, which is equivalent to calculating the shared area of the unit height pulses. Coherence was defined as the sum of the shared areas divided by the square root of the product of the total areas of each individual train (White *et al.*, 1998; Santhakumar *et al.*, 2005). Average global coherence was calculated from the coherence values obtained for all cell pair combinations using custom NEURON code. In simulations performed with E_{GABA} set to −54 mV, local coherence of 5% of the adjacent neurons in the network was estimated at the same 3 randomly selected regions within each network. Our selection of the time interval for measuring coherence as 20% of the average FS-BC frequency set the minimum coherence to 0.2. Since there was <1% difference in the coherence calculated using the two methods, only the coherence calculated using the Wang-Buzsaki method is reported in the manuscript. Summary data in Figures 3 and 7 and data for 600 pA somatic current injections in Figures 4 and 5 were generated from 3 independent runs with different randomization seeds. 3D mesh plots examining the effect of stimulus intensity on network frequency and coherence (Figs. 4(d), 4(e), 5(d), and 5(e)) were generated based on data from single runs. Physiological and computational data from multiple runs are presented as mean ± s.e.m. One-way and two-way ANOVA were used to analyze data as appropriate (SigmaPlot 12). Significance was set at $p < 0.05$.

RESULTS

The motivation for the current study stems from our recent experimental findings identifying that dentate FS-BCs express tonic, extrasynaptic GABA currents (Yu *et al.*, 2013) in addition to the classic synaptic GABA currents. Moreover, our studies demonstrated that one week after experimental status epilepticus, there is a significant enhancement of tonic GABA current amplitude and a depolarization of GABA reversal potential in dentate FS-BCs (Yu *et al.*, 2013). Since simulation studies have demonstrated that the rapid kinetics of interconnected FS-BCs are important for generation of gamma frequency oscillations (Bartos *et al.*, 2002; Vida *et al.*, 2006), we propose that the presence of, and seizure-induced increase in, tonic GABA currents, as well as changes in GABA reversal potential, would alter the

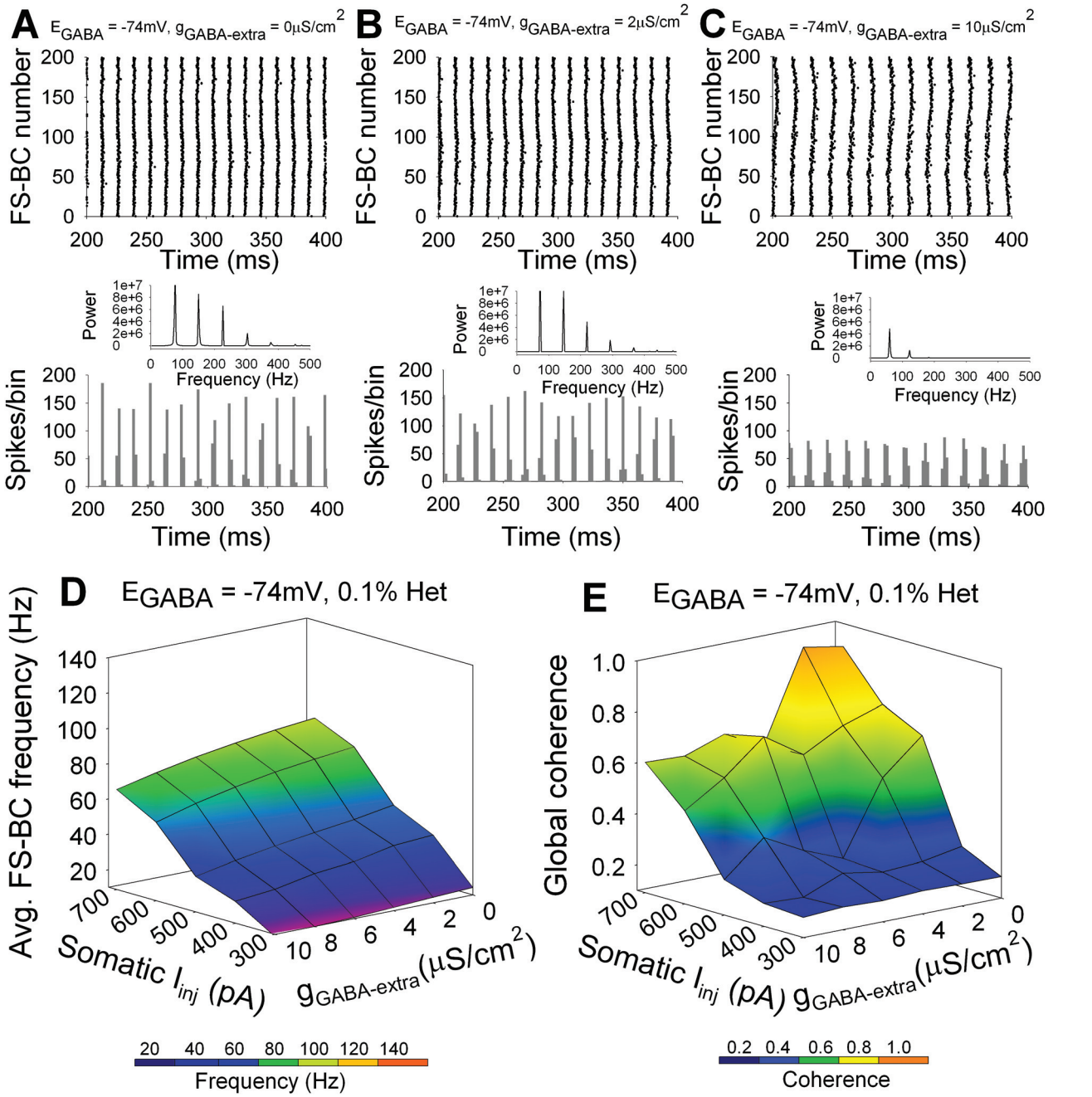

FIG. 4. Effect of extrasynaptic GABA conductance on firing patterns in FS-BC networks activated by somatic current injections. (a)-(c) Spike rasters (top panels) illustrate activity in FS-BC networks with 30 synaptic interconnections and 50 gap junctional connections in which the GABA reversal potential was −74 mV. Networks were activated by a mean somatic current injection of 600 pA with 0.1% heterogeneity, the start time of which was randomly varied between −20 and 50 ms in each cell. Spike rasters in networks simulated with an extrasynaptic GABA conductance of 0 μS/cm^2 (a), 2 μS/cm^2 (b), and 10 μS/cm^2 (c) are illustrated. Corresponding spike-time histograms (bottom panels) show the coherent activity. Insets in bottom panels of (a)-(c) show corresponding frequency power plots. (d) and (e). 3D mesh plot of the average FS-BC frequency (d) and global coherence (e) of FS-BC networks. The mean somatic current injection used to activate the network was systematically varied between 300 and 700 pA with 0.1% heterogeneity (Somatic I_{inj}). Plot shows that effect of increasing tonic GABA conductance ($g_{GABA\text{-}extra}$) from 0 through 10 μS/cm^2.

generation of oscillations in interconnected FS-BC networks. Since the focus of the current study is the dentate gyrus, we consider frequencies in the 40–100 Hz range as gamma frequency oscillations (Bragin *et al.*, 1995). First, we show that the single-cell model FS-BC used in our studies simulated the characteristic passive and active physiology of the biological dentate FS-BCs. We reason that the multicompartmental FS-BC model with biologically based intrinsic properties is ideally suited to implement experimentally based tonic and synaptic conductance values and allows for a more natural segregation of synaptic and gap junctional conductances to different somato dendritic compartments. We then directly examine how introducing gap junctional and tonic GABA conductances, the two conductances that we will incorporate in subsequent simulations, impact the input resistance of our model FS-BC. Next, in the absence of tonic GABA conductance, we investigate whether activity in networks of biologically based FS-BCs, interconnected by

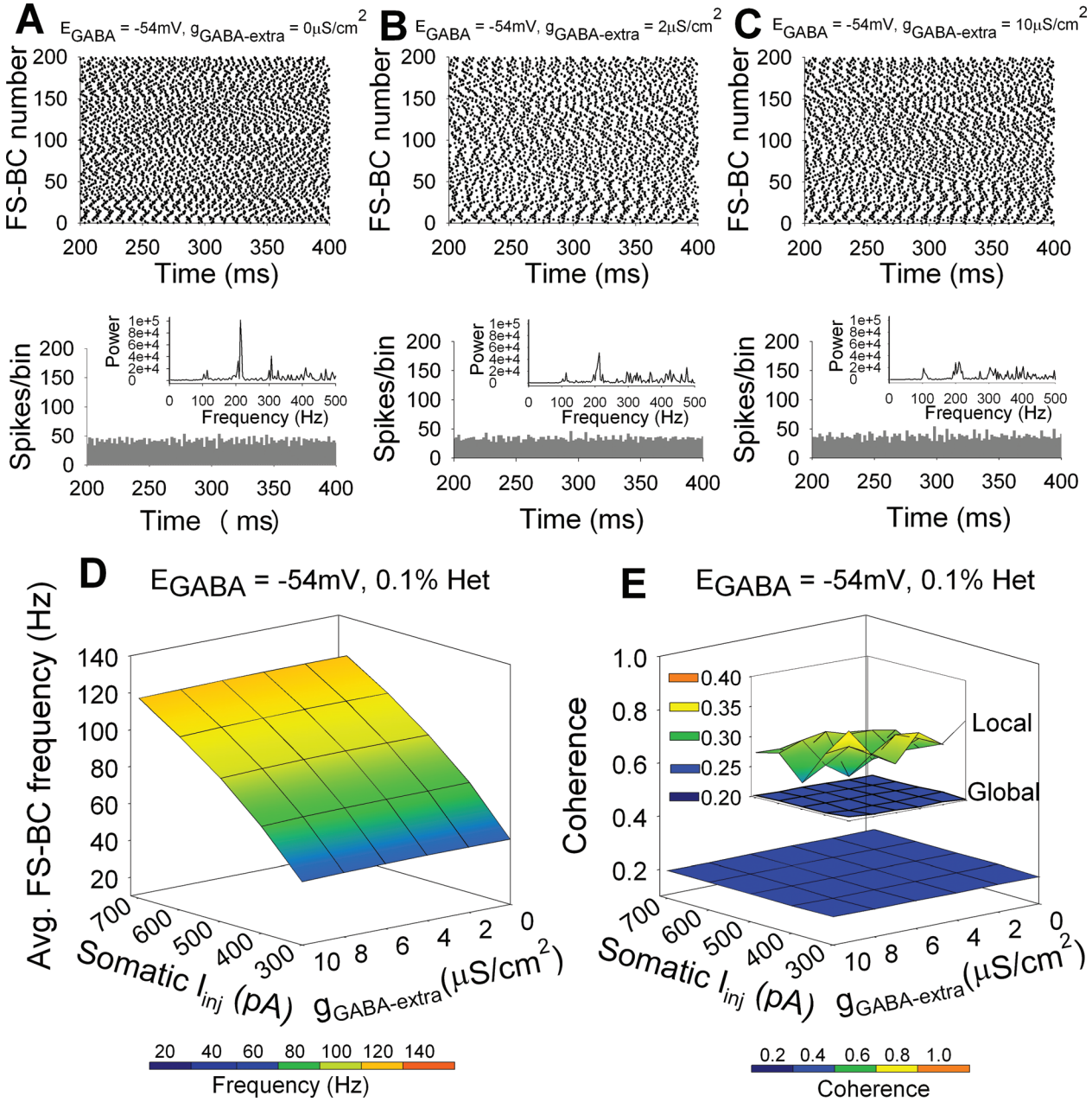

FIG. 5. Extrasynaptic GABA conductance and GABA reversal modulate FS-BC network activity during heterogeneous somatic current injections. (a)-(c). Representative spike rasters (top panels) show activity in FS-BC networks with 30 synaptic interconnections and 50 gap junctional connections and GABA reversal potential set to −54 mV when activated by a mean somatic current injection of 600 pA with 0.1% heterogeneity, the start time of which was randomly varied between −20 and 50 ms in each cell. Spike rasters in networks simulated with an extrasynaptic GABA conductance of 0 μS/cm^2 (a), 2 μS/cm^2 (b), and 10 μS/cm^2 (c) are illustrated. Corresponding spike-time histograms (bottom panels) show the lack of coherent activity. Insets in bottom panels of (a)-(c) show corresponding frequency power plots. (d) and (e). 3D mesh plots show the average FS-BC frequency (D) and global coherence (e) of FS-BC networks with 30 synaptic interconnections and 50 gap junctional connections and GABA reversal potential set to −54 mV. The mean somatic current injection used to activate the network was systematically varied between 300 and 700 pA with 0.1% heterogeneity (somatic I_{inj}). Plot shows the effect of increasing tonic GABA conductance ($g_{GABA\text{-}extra}$) from 0 through 10 μS/cm^2. Inset in (d) compares the global coherence to local coherence in 5% of the network. Legend in (c) applies to (a)-(c).

inhibitory synapses, is modulated by the degree of synaptic interconnectivity, presence of synaptic delay and gap junctional connectivity, as has been demonstrated in earlier studies using networks of generic, single compartment, fast-spiking interneurons (Wang and Buzsaki, 1996; Bartos *et al.*, 2001; Bartos *et al.*, 2002). Following analysis of the baseline activity patterns of the biologically based FS-BC networks, we focus on specific questions concerning how experimentally observed FS-BC tonic GABA currents, status epilepticus-induced increase in tonic GABA currents, and status epilepticus-induced depolarization of GABA reversal potential impact network activity. Specifically, we analyze FS-BC networks with 30 synaptic connections, including distance dependent conduction delay and biologically based dendritic gap junctional coupling to investigate how network activity is altered under the following conditions: (1) introducing tonic GABA conductance at levels that mediate tonic GABA currents observed in FS-BCs from control rats (not subject to status

epilepticus), while maintaining GABA reversal potential at values observed in control rats; (2) progressively increasing tonic GABA conductance in the range reflecting tonic GABA current levels in FS-BCs from rats subject to status epilepticus, while maintaining GABA reversal potential at values observed in control rats; (3) setting the GABA reversal potential to values observed in rats subject to status epilepticus in the absence of tonic GABA currents; and (4) introducing control values of tonic GABA conductance and systematically increasing tonic GABA conductance in the range comparable to FS-BCs from rats subject to status epilepticus, while simultaneously setting the GABA reversal potential to values observed in rats subject to status epilepticus. Network activity was examined in response to somatic current injections at a range of excitatory drives and different heterogeneities, and during biologically based dendritic synaptic inputs. Additionally, since gap junctions act as low pass filters (Gibson *et al.*, 2005) and FS-BCs express gap junctions (Bartos *et al.*, 2001), a subset of networks activated by dendritic synaptic inputs were simulated without gap junctions to examine potential interactions between gap junctions and tonic GABA currents. The simulation results demonstrate that experimentally identified, status epilepticus-induced alterations in FS-BC GABA currents compromise gamma frequency oscillations.

Comparison of model and biological basket cell physiology

The most salient intrinsic biophysical properties of FS-BCs include high frequency non-adapting firing and low input resistance (Hefft and Jonas, 2005; Zhang and Buckmaster, 2009). In order to directly compare the intrinsic properties of the model FS-BC to the biological neurons, we obtained physiological recordings from dentate basket cells. As illustrated in Figure 1, FS-BCs were identified by their morphological features including axon in the granule cell layer, immunoreactivity for parvalbumin (Fig. 1(a)), and characteristic high frequency, non-adapting firing pattern (Fig. 1(c)). We adapted the multi-compartmental basket cell model used in earlier studies (Santhakumar *et al.*, 2005; Dyhrfjeld-Johnsen *et al.*, 2007). The model FS-BC had two apical and 2 basal dendrites each with 4 compartments (Fig. 1(b)). The resting membrane potential of the model FS-BC was set to -75 mV, consistent with that of biological FS-BCs (-74.0 ± 1.9, $n = 10$ cells) reported in our recent study (Yu *et al.*, 2013). In response to positive current injections, the model FS-BC simulated the high frequency, non-adapting firing pattern observed in biological FS-BCs (Figs. 1(c) and 1(d)). Comparison of the model FS-BC firing frequency in response to increasing positive current injections demonstrated that the firing in response to steady state current injections was similar in the model and biological FS-BCs (Fig. 1(e), firing data in biological FS-BCs was obtained from $n = 12$ cells). FS-BCs are known to have a low input resistance compared to other hippocampal interneurons. The input resistance (R_{in}) of the model FS-BC was set to 94.3 MΩ, consistent with the range observed in biological FS-BCs (FS-BC R_{in}: 93.0 ± 10.6 MΩ, $n = 12$ cells, data previously reported in Yu *et al.*, 2013). Since neuronal R_{in} can modify both responses to current injections and how synaptic and extrasynaptic conductances impact neuronal excitability, we reason that the use of the model neurons tuned to replicate FS-BC input resistance is ideally suited to investigate the effect of biologically based extra synaptic GABA conductance values. Moreover, the use of multi-compartmental models allows for a more biologically based segregation of synaptic and gap junctional conductances to different compartments.

Effect of gap junctional and extrasynaptic GABA conductance on FS-BC input resistance

In addition to synaptic connections, FS-BC networks are interconnected by electrical synapses. A majority of subsequent network simulation included gap junctions connections between 50 neighboring FS-BCs, each with a biophysically based single channel conductance of 10 pS (Srinivas *et al.*, 1999). In order to determine whether the inclusion of the gap junctional conductance altered FS-BC input resistance, we systematically increased the conductance of a single gap junction between a pair of FS-BCs and measured the input resistance. Since gap junctions are located in dendrites (Amitai *et al.*, 2002), we considered the two extreme conditions, distributing all gap junctional conductances in either the proximal (1°) or distal (4°) dendritic compartments. Regardless of whether gap junctions were all located in the proximal or distal dendritic compartment, junctional conductances in the range of 1 to 100 pS did not decrease FS-BC input resistance (Fig. 2(a)). Additional increases in junctional conductance progressively reduced FS-BC input resistance to 90.3 MΩ at the 500 pS gap junctional conductance introduced in the model FS-BCs in our network simulations (Fig. 2(a)).

Next, we introduced baseline $g_{GABA\text{-}extra}$ as a deterministic conductance uniformly distributed in all somatic and dendritic compartments. The magnitude of the specific membrane conductance was varied between 2 and 10 $\mu S/cm^2$, the conductance range that was estimated to simulate the biologically relevant range (10 to 60 pA) of extrasynaptic GABA currents (Yu *et al.*, 2013). Varying the $g_{GABA\text{-}extra}$ across this entire range resulted in a $< 10\%$ change in FS-BC input resistance (Fig. 2(b)). Moreover, including an additional 500 pS gap junctional conductance did not alter FS-BC input resistance beyond that resulting from the $g_{GABA\text{-}extra}$. Thus, the non-synaptic conductances introduced into model FS-BCs in the subsequent network simulation are not likely to result in major changes in FS-BC passive membrane properties.

Effect of synaptic interconnectivity on network oscillations

We used networks of 200 FS-BCs connected in a virtual ring (Bartos *et al.*, 2002; Vida *et al.*, 2006) to examine how the degree of GABAergic synaptic interconnectivity affects network oscillations (Wang and Buzsaki, 1996; Bartos *et al.*, 2001; Bartos *et al.*, 2002). Since the aim of the simulations was to determine if activity in networks of biologically based FS-BCs were similar to those observed in earlier interneuronal network models (Bartos *et al.*, 2001; Bartos *et al.*, 2002), these simulations did not include $g_{GABA\text{-}extra}$. Several earlier

studies examining network oscillations have implemented networks activated by somatic current injections (Wang and Buzsaki, 1996; Bartos *et al.*, 2001). However, biological networks are activated by excitatory synaptic inputs to the dendrites. Therefore, we considered two conditions: (1) networks activated by somatic current injection to allow for comparison of results with earlier simulation studies, and (2) networks with biologically based excitatory synaptic inputs to the distal (4°) dendrites constrained by experimentally determined synaptic parameters (Yu *et al.*, 2013) to simulate biological inputs. We first consider networks activated by somatic current injections before analyzing networks activated by with biologically based dendritic excitatory synaptic inputs. We progressively increased the number FS-BCs connected by inhibitory synapses from 4 to 100 (a range of 5% to 50% network connectivity). Synaptic conductance and kinetics were constrained by experimental data (Santhakumar *et al.*, 2005) and held constant in all simulations. Individual FS-BCs in the network were activated by a homogeneous 600 pA somatic current injection, which was initiated at different time points to introduce asynchrony (see Methods). In order to allow for direct comparison between the firing patterns in networks activated by somatic current injections and dendritic synaptic inputs, somatic current injection was tuned such that the average FS-BC frequency in unconnected networks activated by somatic current injections and dendritic synaptic inputs was similar (see Fig. 3(c), with 0 FS-BC synapses, the average FS-BC frequency in Hz: somatic 600 pA current injection: 82.3, dendritic synaptic inputs: 83.2).

In networks activated by a homogeneous 600 pA current injection, increasing FS-BC connectivity lead to an initial decrease in average FS-BC frequency from 73.73 ± 0.11 Hz with 4 connections to 49.7 ± 0.01 Hz when each FS-BC was connected to 30 neighbors (Figs. 3(a) and 3(c)) followed by an increase back to 70.84 ± 0.07 Hz when FS-BCs contacted 40 or more neighbors (Fig. 3(c), $F_{(6,28)} = 7.7$, $p < 0.05$ for effect of FS-BC interconnections by two-way ANOVA examining effect of network input type and FS-BC interconnections, based on $n = 3$ runs). Notably, regardless of the connectivity, the average FS-BC frequency remained within the dentate gamma frequency range (40-100 Hz). Unlike frequency, coherence, which is a measure of synchronous network firing, was relatively low when FS-BCs contacted fewer than 20 neighbors and increased when 20 or more FS-BCs were connected (Fig. 3(d), $F_{(6,28)} = 151.3$, $p < 0.05$ for effect of FS-BC interconnections by two-way ANOVA examining effect of network input type and FS-BC interconnections, based on $n = 3$ runs). Networks in which 70 or more FS-BCs were interconnected showed robust synchrony in firing as observed in earlier studies (Wang and Buzsaki, 1996), possibly because the FS-BCs were activated by homogeneous somatic current injections.

Next, we examined whether the extent of GABAergic synaptic interconnectivity alters network activity when FS-BCs are activated by biologically based dendritic synaptic inputs. Perforant path based AMPA synapses were located on the apical distal (4°) dendrites of FS-BCs and activated by Poisson-distributed spike trains at an average frequency of 200 Hz. Networks within the wide range of GABAergic synaptic interconnectivity (4 to 100 FS-BC interconnections) synchronized in the range of 40-80 Hz. Interestingly, even though the average FS-BC frequency was similar in unconnected networks, the average FS-BC frequency of synaptically activated networks, in which 20 and 30 FS-BCs were interconnected, was higher than that observed in networks activated by somatic current injections (Figs. 3(a)–3(c)). Statistical comparison revealed significance for effects of input type (effect of somatic current injection versus dendritic synaptic inputs on frequency: $F_{(1,28)} = 28.3$, $p < 0.05$), number of FS-BC synaptic interconnections (effect of FS-BC interconnections on frequency: $F_{(6,28)} = 7.74$, $p < 0.05$) and interaction between FS-BC synaptic interconnections and input type ($F_{(6,28)} = 12.24$, $p < 0.05$, by two-way ANOVA) on average FS-BC frequency. While the overall effect of input type on coherence of FS-BC firing was not statistically significant ($F_{(1,28)} = 0.26$, $p > 0.05$, by two-way ANOVA), the number of FS-BC synaptic interconnections ($F_{(6,28)} = 151.26$, $p < 0.05$) and interaction between FS-BC synaptic interconnections and input type ($F_{(6,28)} = 35.9$, $p < 0.05$, by two-way ANOVA) showed statistically significant effects. Moreover, in networks with 20 and 30 FS-BC interconnections, there was a significant differences in both frequency and coherence between networks activated by somatic current injections and dendritic synaptic inputs (by pairwise multiple comparison using Bonferroni t-test). It is possible that the dendritic synaptic input, developed based on the biological perforant path inputs from the entorhinal cortex contribute to the higher average FS-BC frequency in synaptically activated networks as has been identified *in vivo* (Bragin *et al.*, 1995). FS-BC networks activated by excitatory dendritic synaptic inputs synchronized with fewer FS-BC synaptic interconnections. Synaptically activated networks in which FS-BCs connected to 20 to 40 neighbors showed considerably higher coherence than structurally similar networks activated by constant current injection in FS-BCs (Fig. 3(d), $p < 0.05$ by pairwise multiple comparison using Bonferroni t-test). Overall, coherence in synaptically activated networks remained relatively stable when 20 or more FS-BCs were interconnected by fast GABA synapses. The ability of the network to attain stable coherence when FS-BCs contact 20 or more neighbors is of particular interest since, based on morphological data (Sik *et al.*, 1997; Bartos *et al.*, 2001), basket cells in the dentate gyrus are estimated to contact approximately 35 neighboring basket cells (Dyhrfjeld-Johnsen *et al.*, 2007; Santhakumar, 2008). Thus, it appears that the dentate basket cell networks may have an optimal connectivity to support coherent network oscillations.

Earlier studies using networks of generic fast-spiking model neurons activated by somatic current injections have indicated that the presence of distance dependent axonal conduction delay and gap junctional coupling can modulate network coherence (Bartos *et al.*, 2002; Bartos *et al.*, 2007). In networks activated by somatic current injections, inclusion of distance dependent conduction delay resulted in an increase in firing frequency (Fig. 3(e), $p < 0.05$ for effect on delay in networks with 30 FS-BC interconnections by

pairwise multiple comparison using Holm-Sidak method) and coherence (Fig. 3(f), $p < 0.05$ for effect on delay in networks with 30 FS-BC interconnections by pairwise multiple comparison using Holm-Sidak method) in networks with 30 interconnections. However, the change in frequency and coherence in networks with higher interconnections was marginal (Figs. 3(e) and 3(f)). Thus, overall, the increase in frequency and coherence failed to reach statistical significance (frequency: $F_{(2,42)} = 3.02$, $p > 0.05$, coherence: $F_{(2,42)} = 2.87$, $p > 0.05$, for effect of FS-BC interconnections by two-way ANOVA examining effect of input type and FS-BC interconnections). These simulation data suggest that conduction delay may result in limited enhancement of synchrony of networks with fewer interconnections. Inclusion of gap junctional connections (distributed in all four dendritic compartments) to 50 neighbors leads to little additional increase in firing frequency (Fig. 3(e)) or coherence (Fig. 3(f)) in networks with 30 or more connections (frequency: $F_{(2,42)} = 3.02$, $p > 0.05$, coherence: $F_{(2,42)} = 2.87$, $p > 0.05$, for effect of FS-BC interconnections by two-way ANOVA examining effect of input type and FS-BC interconnections). The limited effect of gap junctions on network coherence in our simulations differs from the more robust increase in coherence reported previously (Bartos *et al.*, 2002). It is possible that the use of a single compartmental model with synapses and gap junctions located in the same somatic compartment (Bartos *et al.*, 2002), rather than a biologically based distribution of gap junctions among the dendritic compartments in the current study, contributed to the difference in the magnitude of gap junctional modulation coherence in the 40-80 Hz range. In networks activated by dendritic synaptic inputs, inclusion of conduction delay and gap junctional coupling had negligible effect on either the firing frequency or coherence at all levels of FS-BC connectivity examined (data not shown). However, biological FS-BC networks have gap junctional coupling and conduction delays. Therefore, we proceeded to use homogeneous FS-BC networks including distance-dependent axonal conduction delay, biologically based gap junctional coupling, and 30 synaptic connections between FS-BCs to investigate the effect of $g_{GABA\text{-}extra}$ on network firing and coherence in the two types of networks simulated in this study: (1) networks activated by somatic current injections, and (2) networks activated by dendritic synaptic inputs.

Effect of extrasynaptic GABA currents and GABA reversal on firing patterns of networks activated by somatic current injections

Earlier simulation studies have demonstrated the crucial role played by synaptic inhibition in mediating synchronous gamma frequency oscillations (Wang and Buzsaki, 1996; Bartos *et al.*, 2002; Vida *et al.*, 2006). Experimental data suggest that reduction in interneuronal extrasynaptic GABA currents can increase the frequency of carbachol-induced gamma oscillations *in vitro* through mechanisms involving NMDA receptors (Mann and Mody, 2010). We recently identified the presence of extrasynaptic GABA currents in dentate FS-BCs (Yu *et al.*, 2013). However, whether the presence of extrasynaptic GABA currents in FS-BCs modulates the frequency and coherence of network oscillations has not been tested. Therefore, we examined whether introducing baseline and spillover $g_{GABA\text{-}extra}$ in model FS-BCs modified network oscillations. FS-BCs were connected to 30 adjacent neighbors by GABAergic synapses, as well as 50 local neighbors by dendritic gap junctional connections and were activated by heterogeneous somatic current injections. Mean somatic current injection was systematically varied between 300 and 700 pA with 0.1% heterogeneity to generate 34.3%-10.8% heterogeneity in FS-BC firing in unconnected networks. GABA reversal was set to −74 mV, the experimentally determined value in control FS-BCs (Yu *et al.*, 2013). Multiple simulation runs were performed on networks activated by a mean somatic current injection of 600 pA with 0.1% heterogeneity to allow for statistical comparisons with networks activated by dendritic synaptic inputs. Compared to simulations without extrasynaptic GABA, introducing the normal biological level of baseline $g_{GABA\text{-}extra}$ ($2\,\mu S/cm^2$) and corresponding spillover $g_{GABA\text{-}extra}$ (see Methods) led to a decrease in average FS-BC frequency (Figs. 4(a), 4(b), and 4(d); average FS-BC frequency in Hz when network was activated by 600 pA mean somatic current injection with 0.1% heterogeneity resulting in 12.64% heterogeneity in FS-BC firing in an unconnected network: 73.91 ± 0.65 Hz without $g_{GABA\text{-}extra}$ and 71.31 ± 0.8 Hz with $2\,\mu S/cm^2$ baseline $g_{GABA\text{-}extra}$, $F_{(5,12)} = 102.8$, $p < 0.05$ for effect of $g_{GABA\text{-}extra}$ by one-way ANOVA, $p < 0.05$ by pairwise multiple comparison using Bonferroni t-test, based on $n = 3$ runs each). The decrease in coherence under these conditions did not reach statistical significance (Figs. 4(a), 4(b), and 4(e), coherence when FS-BCs were activated by 600 pA mean somatic current injection with 0.1% heterogeneity: 0.632 ± 0.08 without $g_{GABA\text{-}extra}$ and 0.537 ± 0.13 with $2\,\mu S/cm^2$ baseline $g_{GABA\text{-}extra}$, $F_{(5,12)} = 4.4$, $p < 0.05$ for effect of $g_{GABA\text{-}extra}$ by one-way ANOVA, $p > 0.05$ by pairwise multiple comparison using Bonferroni t-test, based on $n = 3$ runs each). As illustrated by the spike-time histograms in Figures 4(a) and 4(b) (lower panels), all 200 cells fired almost synchronously with no out of phase activity. Indeed, the network frequency under these conditions was similar to the average FS-BC frequency (network frequency in Hz when network was activated by 600 pA mean somatic current injection with 0.1% heterogeneity 76.67 without $g_{GABA\text{-}extra}$ and 73.33 with $2\,\mu S/cm^2$ baseline $g_{GABA\text{-}extra}$). Overall, statistical analysis of data from networks activated by 600 pA mean somatic current injection with 0.1% heterogeneity revealed a significant effect of $g_{GABA\text{-}extra}$ on both average FS-BC frequency ($F_{(5,12)} = 102.8$, $p < 0.05$ by one-way ANOVA) and coherence ($F_{(5,12)} = 4.4$, $p < 0.05$ one-way ANOVA) when E_{GABA} was −74 mV. In simulations where the mean somatic current injection to FS-BCs was systematically varied, networks activated by a mean somatic current injection of 500 pA and above developed coherent firing at frequencies over 40 Hz, in the gamma frequency range, in the absence of tonic GABA conductance (Figs. 4(b)–4(e)). Introducing a baseline $g_{GABA\text{-}extra}$ of $2\,\mu S/cm^2$, consistently decreased the average FS-BC frequency and coherence in networks activated by

somatic current injections (Figs. 4(d) and 4(e)). Additional simulations were conducted in networks activated by mean somatic current injection between 300 and 700 pA and 0.5% heterogeneity to generate a 186.4%-54.6% heterogeneity in FS-BC firing. When the heterogeneity in current injection was increased to 0.5%, the average FS-BC frequency and coherence were reduced from that observed at identical mean somatic current injections and 0.1% heterogeneity possibly due to 12% to 50% of FS-BCs failing to reach firing threshold during the entire simulation period when the mean somatic current injection was 700 and 300 pA, respectively (see Methods). Still, networks activated by a mean somatic current injection of 500 pA and above developed activity in the gamma frequency range (40–80 Hz) with modest coherence (0.3 to 0.35) in the absence of tonic GABA currents (Supplementary Figs. 1(a) and 1(b)). Even with 0.5% heterogeneity, tonic GABA conductance reduced average FS-BC frequency (Supplementary Fig. 1(a), average FS-BC frequency when FS-BCs were activated by 600 pA mean somatic current injection with 0.5% heterogeneity: 63.4 Hz without $g_{GABA\text{-}extra}$ and 55.56 Hz with 2 $\mu S/cm^2$ baseline $g_{GABA\text{-}extra}$) and coherence (Supplementary Fig. 1(b), coherence when FS-BCs were activated by 600 pA mean somatic current injection with 0.5% heterogeneity: 0.35 without $g_{GABA\text{-}extra}$ and 0.29 with 2 $\mu S/cm^2$ baseline $g_{GABA\text{-}extra}$). Interestingly, increasing baseline $g_{GABA\text{-}extra}$ did not alter average FS-BC frequency and coherence in the absence of spillover $g_{GABA\text{-}extra}$ (data not shown), indicating that changes in synaptic decay kinetic resulting from compound spillover synaptic events underlie the effect of tonic GABA currents on network activity patterns. This is consistent with earlier studies demonstrating that decay kinetics of compound inhibitory events can impact network frequency (Fisahn *et al.*, 1998; Brunel and Wang, 2003).

Since we have previously shown that extrasynaptic GABA currents in FS-BCs are enhanced following experimental status epilepticus in rats (Yu *et al.*, 2013), we next examined how progressively increasing extrasynaptic GABA currents impacts network activity. Increasing FS-BC baseline and spillover $g_{GABA\text{-}extra}$ from the levels observed in FS-BCs from control rats (2 $\mu S/cm^2$ baseline $g_{GABA\text{-}extra}$ and corresponding spillover $g_{GABA\text{-}extra}$) resulted in progressive decrease in average FS-BC frequency and an overall decrease in coherence (Figs. 4(b) and 4(e), in networks activated by 600 pA somatic current injection with 0.1% heterogeneity, average FS-BC frequency in Hz, 71.31 ± 0.8 with 2 $\mu S/cm^2$ and 55.34 ± 0.7 with 10 $\mu S/cm^2$ baseline $g_{GABA\text{-}extra}$ based on $n = 3$ runs each, $F_{(5,24)} = 102.8$, $p < 0.05$ for effect of $g_{GABA\text{-}extra}$ on average FS-BC frequency by one-way ANOVA; network coherence, 0.54 ± 0.13 with 2 $\mu S/cm^2$ and 0.46 ± 0.02 with 10 $\mu S/cm^2$ baseline $g_{GABA\text{-}extra}$ based on $n = 3$ runs each, $F_{(5,12)} = 4.4$, $p < 0.05$ for effect of $g_{GABA\text{-}extra}$ coherence by one-way ANOVA). Introducing tonic GABA conductance consistently decreased both frequency and coherence in networks activated by mean somatic current injections in the range of 300 and 700 pA with 0.1% heterogeneity (Figs. 4(d) and 4(e)). When the heterogeneity in current injection was increased to 0.5%, increasing tonic GABA currents reduced average FS-BC frequency to < 30 Hz when the mean somatic current injection was < 500 pA and abolished global network coherence at all current injections examined (Supplementary Figs. 1(a) and 1(b)). Spike-time histogram of most networks activated by 300–700 pA current injections at both 0.1% and 0.5% heterogeneities showed synchronous firing, resulting in similar values for network and average FS-BC frequency. Thus, as with average FS-BC frequency, increasing $g_{GABA\text{-}extra}$ decreased network frequency as well (Supplementary Figs. 2(a) and 2(c)). However, in a few networks, a sub-population of neurons showed out-of-phase activity (spike-time histograms not shown), resulting in approximately doubling of network frequency compared to average FS-BC frequency under these conditions (Supplementary Figs. 2(a) and 2(c)). Since each FS-BC was connected to 30 adjacent FS-BCs by inhibitory synapses and 50 neighboring FS-BCs by gap junctions, there was little variability in network connectivity patterns between simulations. Thus, it appears that the differences in FS-BC firing patterns between different runs resulted in the development of two independently oscillating FS-BC populations in some, but not all, networks.

Apart from an increase in extrasynaptic GABA currents, FS-BC E_{GABA} shifts to values more depolarized than the resting membrane potential after status epilepticus (Yu *et al.*, 2013). Earlier simulation studies have established that E_{GABA} modulates activity of interneuronal networks (Vida *et al.*, 2006; Bartos *et al.*, 2007). Therefore, we examined the effect of altering E_{GABA} on synaptically coupled networks of FS-BCs in the absence of extrasynaptic GABA currents. In networks activated by the somatic current injection, altering synaptic GABA reversal from −74 mV, the value observed in control FS-BCs, to −54 mV, the experimentally measured E_{GABA} in FS-BCs after status epilepticus, increased average FS-BC frequency (compare Figs. 4(a), 5(a), 4(d), and 5(d), average FS-BC frequency in Hz when FS-BCs were activated by 600 pA somatic current injection with 0.1% heterogeneity: 73.9 ± 0.65 with −74 mV E_{GABA}, 105.14 ± 0.05 with −54 mV E_{GABA}, $F_{(1,12)} = 19392.7$, $p < 0.05$ for effect of E_{GABA} by two way ANOVA for effect of E_{GABA} and $g_{GABA\text{-}extra}$ followed by pairwise multiple comparison using Bonferroni t-test) and decreased the coherence (compare Figs. 4(a), 5(a), 4(e), and 5(e), coherence when FS-BCs were activated by 600 pA somatic current injection with 0.1% heterogeneity: 0.63 ± 0.08 with −74 mV E_{GABA}, 0.203 ± 0.0 with −54 mV E_{GABA}, $F_{(1,24)} = 686.3$, $p < 0.05$ for effect of E_{GABA} by two way ANOVA for effect of E_{GABA} and $g_{GABA\text{-}extra}$ followed by pairwise multiple comparison using Bonferroni t-test). Curiously, the increase in average FS-BC frequency occurred even though an E_{GABA} of −54 mV is negative to the model FS-BC firing threshold of −52 mV. The low network coherence of 0.2 in networks with −54 mV E_{GABA} corresponds to an asynchronous activity since our measure of coherence sets the minimum to 0.2 (see Methods). Moreover, although the spike-time histograms and coherence measures showed little coherent activity, the frequency power plot showed a maximum at approximately double the average FS-BC frequency, indicating the presence of local sub networks of oscillations when E_{GABA} is −54 mV (Fig. 5(a) inset in bottom panel, networks without $g_{GABA\text{-}extra}$ and −54 mV

E_{GABA} activated by 600 pA somatic current injection with 0.1% heterogeneity: average FS-BC frequency: 105.14 ± 0.05 Hz; network frequency: 213.33 Hz). For all values of mean current injection examined, altering synaptic GABA reversal from −74 mV to −54 mV increased average FS-BC frequency by over 30 Hz (compare Figs. 4(a), 5(a), 4(d), and 5(d), $F_{(1,24)} = 19392$, $p < 0.05$ for effect of E_{GABA} by two-way ANOVA for effect of E_{GABA} and $g_{GABA\text{-}extra}$ followed by pairwise multiple comparison using Bonferroni t-test), network frequency by 50–100 Hz (Supplementary Figs. 2(a) and 2(b), $F_{(1,24)} = 164474.8$, $p < 0.05$ for effect of E_{GABA} by two-way ANOVA for effect of E_{GABA} and $g_{GABA\text{-}extra}$ followed by pairwise multiple comparison using Bonferroni t-test) and abolished global coherence (compare Figs. 4(a), 5(a), 4(e), and 5(e), $F_{(1,24)} = 686.3$, $p < 0.05$ for effect of E_{GABA} by two-way ANOVA followed by pairwise multiple comparison using Bonferroni t-test). The frequency power plot of the spike-time histogram showed peaks at harmonics of the average FS-BC frequency with the maximum power at twice the average FS-BC frequency (Figs. 5(a)–5(c) inset in bottom panel). Consistent with the presence of a defined peak in the frequency power plot (Figs. 5(a)–5(c) inset in bottom panel), although global coherence indicated that networks with −54 mV E_{GABA} were asynchronous, local coherence in 5% of the network was significantly higher than the global coherence (coherence when FS-BCs activated by 600 pA somatic current injection with 0.1% heterogeneity at −54 mV E_{GABA}, local: 0.27 ± 0.01; global: 0.2 ± 0.0, $F_{(2,18)} = 4404.2$, $p < 0.05$ for effect of local versus global measurement on coherence, $F_{(5,18)} = 13.8$, $p < 0.05$ for effect of $g_{GABA\text{-}extra}$ and $F_{(10,18)} = 14.3$, $p < 0.05$ for interaction between effect of $g_{GABA\text{-}extra}$ and local versus global measurement on coherence by two-way ANOVA followed by pairwise multiple comparison using Bonferroni t-test, based on $n = 3$ runs each) indicating focal areas of coherence. Inclusion of $g_{GABA\text{-}extra}$ observed in FS-BCs from control rats resulted in little change in average FS-BC frequency (Figs. 5(a), 5(b), and 5(d), average FS-BC frequency in Hz when FS-BCs were activated by 600 pA somatic current injection with 0.1% heterogeneity: 105.14 ± 0.05 without $g_{GABA\text{-}extra}$ and 105.12 ± 0.17 Hz with 2 μS/cm^2 $g_{GABA\text{-}extra}$, $F_{(5,12)} = 55.04$, $p < 0.05$ for effect of E_{GABA} by one-way ANOVA, and $p > 0.05$ by pairwise multiple comparison using Bonferroni t-test). Average FS-BC frequency (Fig. 5(d)) remained unchanged with the introduction of $g_{GABA\text{-}extra}$ regardless of the mean somatic current injection used to activate the network. Similarly, average FS-BC frequency was not altered with the introduction of $g_{GABA\text{-}extra}$ in networks activated by somatic current injections with 0.5% heterogeneity (Supplementary Figs. 1(c) and 1(d)). The effect of $g_{GABA\text{-}extra}$ on network frequency was varying, showing no change or a decrease if network frequency was twice the average FS-BC frequency (Supplementary Figs. 2(b) and 2(d)). Thus, our simulations indicate that, even without tonic GABA currents, status epilepticus-induced changes in FS-BC GABA reversal can enhance average FS-BC frequency and compromise coherence.

Next, we examined how increasing FS-BC $g_{GABA\text{-}extra}$, as has been observed status epilepticus, further altered network activity when E_{GABA} was maintained at −54 mV, the value observed in FS-BCs after status epilepticus. Progressively, increasing FS-BC $g_{GABA\text{-}extra}$ caused a marginal decrease in average FS-BC frequency (Figs. 5(b)–5(d) average FS-BC frequency in Hz when FS-BCs were activated by 600 pA somatic current injection with 0.1% heterogeneity: 105.12 ± 0.17 with 2 μS/cm^2 and 103.78 ± 0.04 Hz with 10 μS/cm^2 $g_{GABA\text{-}extra}$). Similarly, increasing FS-BC $g_{GABA\text{-}extra}$ caused a marginal decrease in network frequency (Figs. 5(b) and 5(c) and Supplementary Fig. 2(b), network frequency in Hz when FS-BCs were activated by 600 pA somatic current injection with 0.1% heterogeneity: 213.33 with 2 μS/cm^2 and 210.0 Hz with 10 μS/cm^2 $g_{GABA\text{-}extra}$, $F_{(5,12)} = 55.04$, $p < 0.05$ for effect of $g_{GABA\text{-}extra}$, by one-way ANOVA $p < 0.05$ by pairwise multiple comparison using Bonferroni t-test). Moreover, global coherence of FS-BC firing was consistently lower and comparable to that of unconnected networks when E_{GABA} was −54 mV (Fig. 5, global coherence when FS-BCs were activated by 600 pA somatic current injection with 0.1% heterogeneity: 0.204 in an unconnected network, 0.203 ± 0.0 with 2 μS/cm^2 and 0.204 ± 0.0 with 10 μS/cm^2 $g_{GABA\text{-}extra}$, $F_{(5,12)} = 0.91$, $p > 0.05$ for effect of $g_{GABA\text{-}extra}$, by one-way ANOVA). Even when activated by a range of mean somatic current injections over 300–700 pA with 0.1% heterogeneity, average FS-BC frequency was increased by over 30 Hz when E_{GABA} was depolarized to −54 mV from −74 mV and showed little global coherence in firing (Figs. 4(e) and 5(e)). However, the local coherence measured in 5% of the network was consistently higher than the global coherence (Fig. 5(e) inset, $F_{(2,18)} = 4404.2$, $p < 0.05$ for effect of local versus global measurement on coherence by two-way ANOVA for effect of local versus global measurement and $g_{GABA\text{-}extra}$ followed by pairwise multiple comparison using Bonferroni t-test), indicating focal areas of coherent high frequency (80–220 Hz) network activity when E_{GABA} was depolarized to −54 mV. Even when heterogeneity of the somatic current injections was increased to 0.5%, depolarizing E_{GABA} to −54 mV enhanced the average FS-BC frequency and abolished global coherence (Supplementary Figs. 1(c) and 1(d)), as observed in networks with 0.1% heterogeneity. Unlike networks where E_{GABA} was −74 mV, even with 0.5% heterogeneity, all FS-BCs remained active when the mean somatic current injection was 700 and 400 pA, and only 12% of FS-BCs were inactive when the mean somatic current injection was 300 pA when E_{GABA} was depolarizing. Overall, the network frequency was more variable than the average FS-BC frequency (Supplementary Figs. 2(b) and 2(d)). As illustrated by the frequency power plots of the representative spike-time rasters in the top panels of Figures 5(a)–5(c), there were multiple peaks at harmonics of the average FS-BC frequency and additional high frequency peaks (Figs. 5(a)–5(c) insets in bottom panels). The frequency at which the maximum power was observed fluctuated between the harmonics of the average FS-BC frequency in the network (Supplementary Figs. 2(b) and 2(d)), possibly due to emergence of different sub networks as a consequence of firing heterogeneity. Thus, increasing tonic GABA currents failed to cause reliable modulation of average network frequency beyond the consistent increase in network frequency

caused by the depolarizing shift in E_{GABA} ($F_{(1,24)} = 19392.7$, $p < 0.05$ by for effect of E_{GABA}, ($F_{(5,24)} = 1.13$, $p > 0.05$ for effect of $g_{GABA\text{-}extra}$, and ($F_{(5,24)} = 0.44$, $p > 0.05$ for interaction between E_{GABA} and $g_{GABA\text{-}}$ by two-way ANOVA).

Overall, when networks with shunting E_{GABA} (−74 mV observed in FS-BCs from control rats) are activated by heterogeneous somatic current injections, increases in FS-BC $g_{GABA\text{-}extra}$ within the biologically relevant range, resulted in a decrease in both average FS-BC frequency and network frequency, as well as global coherence. However, the average FS-BC frequency remained within the 40–80 Hz (gamma frequency) range for mean current injections over 500 pA. In contrast to the effect of conductance, shifting E_{GABA} to a depolarized potential of −54 mV, the reversal potential in FS-BCs from rats subject to status epilepticus increased the average FS-BC frequency of networks activated by mean current injections over 500 pA to the 80–120 Hz range and average network frequency to the 100–250 Hz range. When E_{GABA} was −54 mV, increasing $g_{GABA\text{-}extra}$ did not further enhance firing or decrease the already low global coherence. Statistical analyses revealed significant effects for E_{GABA} ($F_{(1,24)} = 19392.7$, $p < 0.05$ by two-way ANOVA), $g_{GABA\text{-}extra}$ ($F_{(5,24)} = 116.87$, $p < 0.05$ by two-way ANOVA) and for interaction between E_{GABA} and $g_{GABA\text{-}extra}$ ($F_{(5,24)} = 87.5$, $p < 0.05$ by two-way ANOVA) on average FS-BC frequency and coherence ($F_{(1,24)} = 686.4$, $p < 0.05$ for effect of E_{GABA}, $F_{(5,24)} = 4.4$, $p < 0.05$ for effect of $g_{GABA\text{-}extra}$ and $F_{(5,24)} = 4.4$, $p < 0.05$ for interaction between E_{GABA} and $g_{GABA\text{-}extra}$ by two way ANOVA). Together, the simulation data from networks activated by heterogeneous somatic current injections indicate that increases in $g_{GABA\text{-}extra}$, which can occur during endogenous or pharmacological modulation of tonic GABA currents (Brickley and Mody, 2012) can alter gamma frequency oscillations under physiological conditions of shunting inhibition (E_{GABA} of −74 mV). However, the depolarized E_{GABA} (−54 mV) observed after status epilepticus (Yu *et al.*, 2013) undermines global network coherence and shifts firing to higher frequencies regardless of the magnitude of $g_{GABA\text{-}extra}$.

Effect of extrasynaptic GABA currents and GABA reversal on firing patterns of networks activated by dendritic synaptic inputs

Analyses of interneuronal networks activated by somatic current injections have led to major advances in understanding the mechanisms underlying generation of network oscillations (Wang and Buzsaki, 1996; Bartos *et al.*, 2002; Vida *et al.*, 2006). However, biological networks are activated by excitatory synaptic inputs to the dendrites. Therefore, we evaluated whether the modulation of network oscillations by extrasynaptic inhibition and E_{GABA} is altered when FS-BCs were activated by excitatory synaptic inputs to the distal dendrites. Networks of 200 FS-BCs connected to the 30 nearest neighbors by inhibitory synapses and to 50 neighbors by gap junctional coupling were activated by individual 200 Hz trains of Poisson-distributed, simulated perforant path-like distal dendritic synaptic inputs (Yu *et al.*, 2013).

As in networks activated by somatic current injections, introducing the normal biological level of baseline $g_{GABA\text{-}extra}$ (2 $\mu S/cm^2$) and corresponding spillover $g_{GABA\text{-}extra}$ reduced both average FS-BC frequency and coherence (Figs. 6(a) and 6(b) and Figs. 7(a) and 7(b); average FS-BC frequency in Hz: 74.1 ± 0.01 without $g_{GABA\text{-}extra}$ 69.47 ± 1.03 with 2 $\mu S/cm^2$ $g_{GABA\text{-}extra}$; coherence: 0.65 ± 0.0 without $g_{GABA\text{-}extra}$, 0.58 ± 0.02 with 2 $\mu S/cm^2$ $g_{GABA\text{-}extra}$, n = 3 runs, $F_{(5,24)} = 21.02$, $p < 0.05$ for effect of $g_{GABA\text{-}extra}$ on frequency and $F_{(1,24)} = 23.97$, $p < 0.05$ for effect of $g_{GABA\text{-}extra}$ on coherence by two-way ANOVA followed by pairwise multiple comparison using Bonferroni t-test). As expected based on the presence of highly synchronous firing in the spike-time histograms (Figs. 6(a) and 6(b), bottom panels), the network frequency was similar to average FS-BC frequency and decreased with the addition of $g_{GABA\text{-}extra}$ (Fig. 7(c); network frequency in Hz: 76.67 ± 0.0 without $g_{GABA\text{-}extra}$ and 71.1 ± 1.11 with 2 $\mu S/cm^2$ $g_{GABA\text{-}extra}$). Next, we examined how increasing FS-BC extrasynaptic GABA currents to simulate the increase in extrasynaptic GABA currents after status epilepticus (Yu *et al.*, 2013), impacts network activity. Increasing $g_{GABA\text{-}extra}$ resulted in an overall decrease in both average FS-BC and network frequency and global network coherence (Figs. 6(b) and 6(c) and Figs. 7(a) and 7(b); average FS-BC frequency in Hz: 69.47 ± 1.03 with 2 $\mu S/cm^2$ $g_{GABA\text{-}extra}$ and 54.94 ± 0.06 with 10 $\mu S/cm^2$ $g_{GABA\text{-}extra}$; global coherence: 0.58 ± 0.02 with 2 $\mu S/cm^2$ $g_{GABA\text{-}extra}$ and 0.48 ± 0.0 with 10 $\mu S/cm^2$ $g_{GABA\text{-}extra}$, $F_{(5,24)} = 21.02$, $p < 0.05$ for effect of $g_{GABA\text{-}extra}$ on frequency and $F_{(1,24)} = 23.97$, $p < 0.05$ for effect of $g_{GABA\text{-}extra}$ on coherence by two-way ANOVA; network frequency in Hz: 71.1 ± 1.11 with 2 $\mu S/cm^2$ $g_{GABA\text{-}extra}$ and 63.3 ± 0.0 with 10 $\mu S/cm^2$ $g_{GABA\text{-}extra}$). Both networks activated by somatic current injection and those activated by dendritic synaptic inputs synchronized in the 40–80 Hz range, within the gamma frequency range in the dentate (Bragin *et al.*, 1995). Increasing $g_{GABA\text{-}extra}$ decreased the average FS-BC frequency and coherence under both conditions. Additional simulations in which FS-BCs were devoid of gap junctional connections revealed that, regardless of the presence of gap junctions, $g_{GABA\text{-}extra}$ reduced average FS-BC frequency and coherence when E_{GABA} was −74 mV (Figs. 7(a) and 7(b)). Similarly, the ability of increases in $g_{GABA\text{-}extra}$ to decrease average FS-BC frequency and coherence was maintained even when network connectivity was increased to 40 adjacent neighbors (data not shown).

Next, we examined how depolarizing E_{GABA} modulated synchrony in networks activated by biologically based dendritic synaptic inputs. In networks with GABAergic synaptic connections to 30 adjacent FS-BCs simulated without $g_{GABA\text{-}extra}$ and with E_{GABA} set to −54 mV, the average FS-BC frequency was higher, but coherence considerably lower, than similar networks with a −74 mV E_{GABA} (Figs. 6(a), 6(d), 7(a), and 7(b); average FS-BC frequency in Hz: 74.1 ± 0.01 when E_{GABA} was −74 mV and 122.6 ± 0.01 when E_{GABA} was −54 mV, $F_{(1,24)} = 26641$ $p < 0.05$ for effect of E_{GABA} by two-way ANOVA followed by pairwise multiple comparison using Bonferroni t-test; coherence: 0.65 ± 0.0 when E_{GABA} was −74 mV and 0.203 ± 0.0 when E_{GABA} was −54 mV, $F_{(1,24)} = 5662$, $p < 0.05$ for effect of E_{GABA} by two-way ANOVA followed by pairwise multiple comparison using Bonferroni t-test). Even though the

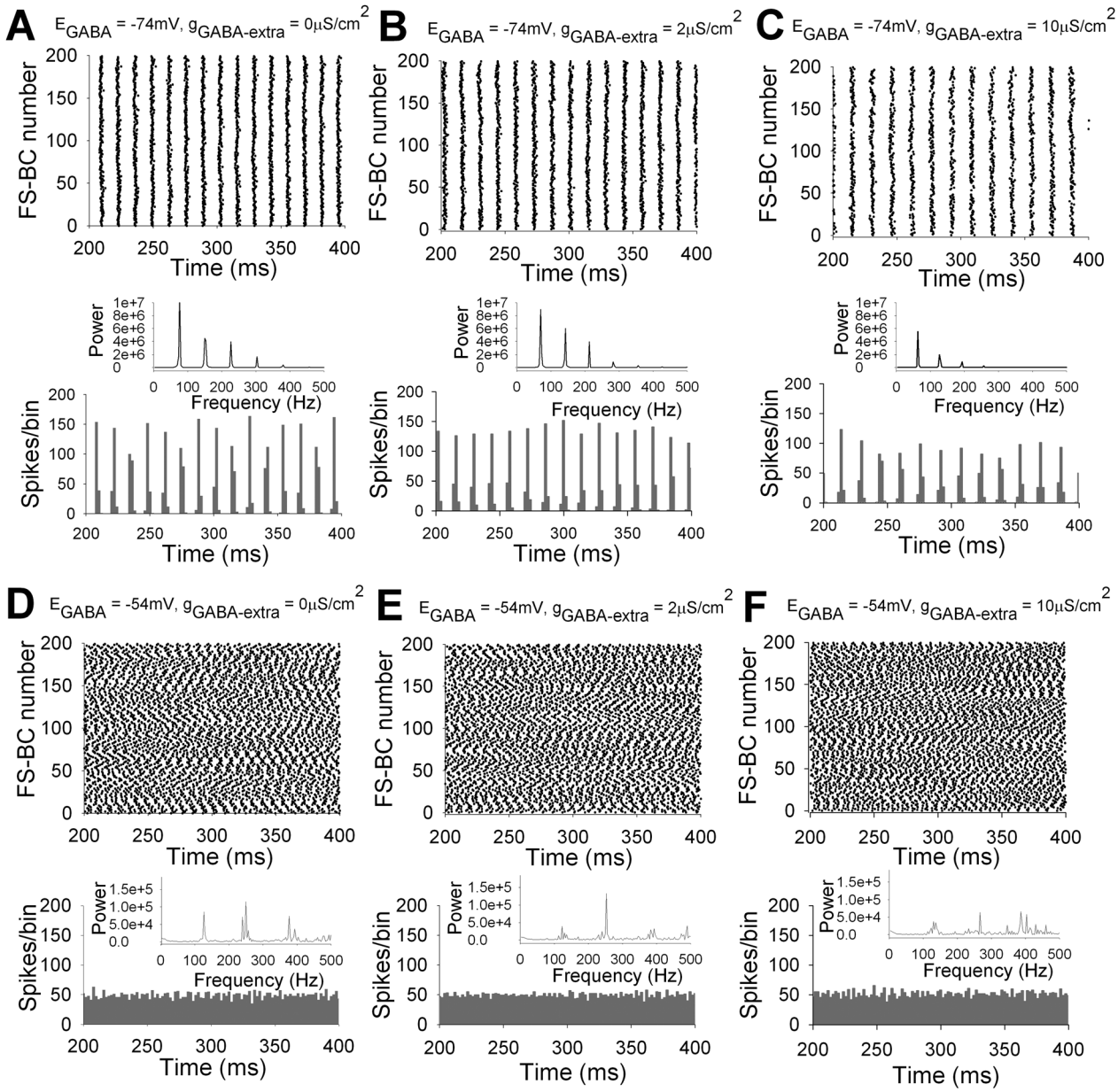

FIG. 6. Effect of extrasynaptic GABA conductance modulates frequency and coherence in networks activated by biologically based dendritic synaptic inputs. (a)-(f) Spike rasters (top panels) of activity in FS-BC networks with synaptic and gap junctional interconnections activated by biologically based dendritic synaptic inputs. Spike rasters in networks simulated with a GABA reversal of −74 mV and extrasynaptic GABA conductance of 0 μS/cm^2 (a), 2 μS/cm^2 (b), and 10 μS/cm^2 (c) and GABA reversal of −54 mV and extrasynaptic GABA conductance of 0 μS/cm^2 (d), 2 μS/cm^2 (e) and 10 μS/cm^2 (f). Corresponding spike-time histograms are shown in the bottom panels. Spike-rater plots for illustrations had a bin width of 2 ms. Insets in bottom panels of (a)-(c) show corresponding frequency power plots.

spike-time histogram showed relatively asynchronous activity when E_{GABA} was set to −54 mV (Fig. 6(d), bottom panel), the frequency power plots (Fig. 6(d), inset) showed peaks at harmonics of the average FS-BC frequency indicating sub-population of neurons with oscillations, and network frequency was increased from 76.67 ± 0.00 Hz when E_{GABA} was −74 mV to 250 ± 0.00 when E_{GABA} was −54 mV ($F_{(1,24)} = 30.4$, $p < 0.05$ for effect of E_{GABA}, $F_{(5,24)} = 0.3$, $p > 0.05$ for effect of $g_{GABA\text{-}extra}$ and $F_{(5,24)} = 0.4$, $p > 0.05$ for interaction between $g_{GABA\text{-}extra}$ and E_{GABA} by two-way ANOVA followed by pairwise multiple comparison using Bonferroni t-test, based on 3 runs each).

Similar to networks activated by somatic current injections, increasing $g_{GABA\text{-}extra}$ progressive enhanced the average FS-BC frequency between 120 and 130 Hz and abolished global network coherence (Figs. 6(e), 6(f), 7(a), and 7(b); average FS-BC frequency in Hz: 123.8 ± 0.01 with 2 μS/cm^2 $g_{GABA\text{-}extra}$ and 130.0 ± 0.0 with 10 μS/cm^2 $g_{GABA\text{-}extra}$, $F_{(5,24)} = 21.02$, $p < 0.05$ for effect of $g_{GABA\text{-}extra}$ by two-way ANOVA with $p < 0.05$ by pairwise multiple comparison using Bonferroni t-test, $F_{(5,24)} = 115.8$, $p < 0.05$ for effect of interaction between E_{GABA} and $g_{GABA\text{-}extra}$ on average FS-BC frequency by two-way ANOVA; coherence: 0.203 ± 0.0 with 2 μS/cm^2 $g_{GABA\text{-}extra}$ and 0.204 ± 0.0 with 10 μS/cm^2 $g_{GABA\text{-}extra}$, $F_{(5,24)} = 23.97$, $p < 0.05$ for effect of $g_{GABA\text{-}extra}$ by two-way ANOVA with $p > 0.05$ by pairwise multiple comparison using Bonferroni t-test, and $F_{(5,24)} = 24.3$, $p < 0.05$ for effect of interaction between E_{GABA} and

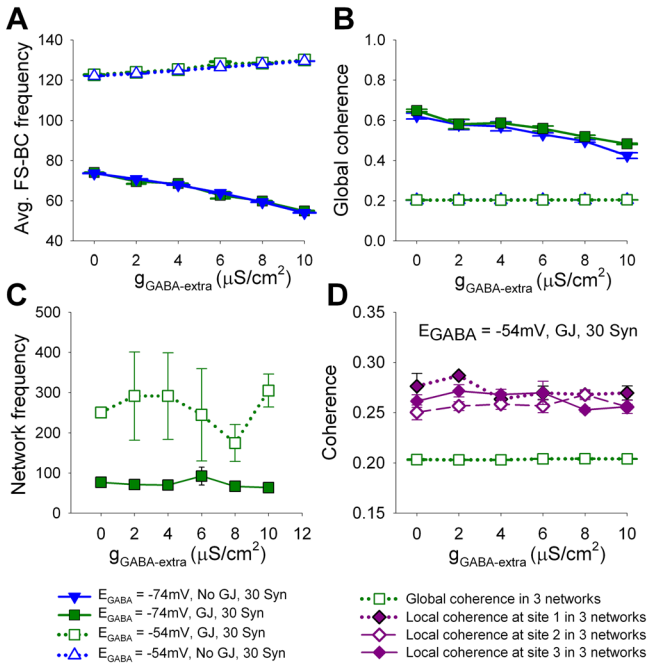

FIG. 7. Summary of the effect of extrasynaptic GABA conductance on activity in FS-BC networks activated by dendritic synaptic inputs. (a)-(c) Summary data from networks activated by dendritic synaptic inputs show the effect of FS-BC tonic GABA conductance on average FS-BC frequency (a) and global coherence (b) and network frequency (c). Legend below (c) applies to (a)-(c). (d) Plot compares the global coherence and local coherence (computed for a local 5% of the network) in synaptically activated networks with a GABA reversal potential set to −54 mV. Local coherence calculated at each site in the network is presented as mean ± s.e.m across three independent network instantiations used to evaluate global coherence. Data are presented as mean ± s.e.m of 3 independent network simulations.

$g_{GABA\text{-}extra}$ on coherence by two-way ANOVA). When E_{GABA} was set to −54 mV, average FS-BC frequency consistently remained over 120 Hz. In contrast to the progressive increase in average FS-BC frequency, the effect of increasing $g_{GABA\text{-}extra}$, on network frequency was variable (Figs. 6(e), 6(f), and 7(c); frequency in Hz: 291.11 ± 109.41 with $2\,\mu S/cm^2$ $g_{GABA\text{-}extra}$ and 304.440 ± 41.16 with $10\,\mu S/cm^2$ $g_{GABA\text{-}extra}$, $F_{(5,24)} = 0.3$, $p > 0.05$ for effect of $g_{GABA\text{-}extra}$ and $F_{(5,24)} = 0.4$, $p > 0.05$ for interaction between $g_{GABA\text{-}extra}$ and E_{GABA} by two-way ANOVA based on 3 runs each). As illustrated by the frequency power plots in the insets of the bottom panels of Figures 6(e) and 6(f), the networks showed peaks at multiple frequencies over 200 Hz including harmonics of the average FS-BC frequency. The harmonic that reflected the peak frequency in the frequency power plot varied considerably between different networks. Consistent with the presence of FS-BC sub networks with oscillations, the local coherence in networks with E_{GABA} set to −54 mV was significantly higher than the corresponding global coherence at all levels of $g_{GABA\text{-}extra}$ (Fig. 7(d), $F_{(1,24)} = 534.6$, $p < 0.05$ for effect of local versus global measurement on coherence by two-way ANOVA followed by pairwise multiple comparison using Bonferroni t-test at all levels of $g_{GABA\text{-}extra}$, $F_{(5,24)} = 1.2$, $p > 0.05$ for effect of $g_{GABA\text{-}extra}$ and $F_{(5,24)} = 1.3$, $p > 0.05$ for interaction between effect of $g_{GABA\text{-}extra}$ local versus global measurement on coherence and by two-way ANOVA) indicating focal areas of modest coherence. In additional simulations where gap junctional connections were excluded (Figs. 7(a) and 7(b)) or when FS-BCs were connected to 40 adjacent neighbors (data not shown), increasing $g_{GABA\text{-}extra}$ steadily enhanced the average FS-BC frequency in the range of high frequency oscillations in the presence of the depolarizing E_{GABA}.

Thus, simulations of networks activated by distal dendritic excitatory synaptic inputs demonstrate that $g_{GABA\text{-}extra}$ can modulate gamma frequency oscillations, reducing frequency and coherence when E_{GABA} is shunting and increasing average FS-BC frequency when E_{GABA} is depolarizing. Furthermore, irrespective of how the networks were activated, the depolarizing shift in FS-BC E_{GABA} enhanced firing to over 120 Hz shifting normal gamma frequency oscillations to the high frequency network activity with low global coherence yet modest local coherence, which could promote epileptic activity.

DISCUSSION

Network simulations have shown that fast-spiking interneurons connected by fast GABA synapses play a role in generation of gamma frequency oscillations in brain networks (Wang and Buzsaki, 1996; Whittington *et al.*, 2000; Bartos *et al.*, 2002; Bartos *et al.*, 2007). Apart from the network structure which can sculpt spatial and temporal patterns of activity (Netoff *et al.*, 2004; Percha *et al.*, 2005; Morgan and Soltesz, 2008), recent reports have underscored the effect of intrinsic neuronal properties on network firing patterns (Tateno and Robinson, 2006; Bogaard *et al.*, 2009; Wang, 2010; Skinner, 2012; Borgers and Walker, 2013). Here, we use homogeneous networks of biophysically based models of dentate fast-spiking basket cells to examine the effect of synaptic interconnectivity and extrasynaptic inhibition on network firing patterns. Simulation results from networks without conduction delay and gap junctional coupling demonstrate that networks with 20-40 synaptic interconnections activated by realistic synaptic current inputs develop more coherent network firing at higher gamma frequency ranges than networks in which model neurons are activated by somatic current injections (Figs. 3(a) and 3(b)). Networks with 30 to 40 synaptic connections, similar to the range of basket cell connectivity estimated based on experimental literature (Dyhrfjeld-Johnsen *et al.*, 2007), develop coherent firing in the 40-80 Hz range, within the gamma frequency spectrum of the dentate gyrus (Bragin *et al.*, 1995). As identified in earlier studies (Bartos *et al.*, 2002), axonal conduction delay has marginal effect on the average FS-BC frequency but enhances the coherence of network activity in the biologically relevant range of FS-BC interconnections. However, gap junctional coupling has negligible effect on both average FS-BC frequency and coherence. In the presence of shunting GABA reversal (−74 mV), extrasynaptic GABA conductance reduces both frequency and coherence of gamma oscillations (Figs. 4, 6(a), 6(c), 7(a), and 7(b) and Supplementary Figs. 1(a), 1(b), and 2(a)), demonstrating that modulation of basket cell tonic inhibition can impact network rhythms. A depolarizing shift in E_{GABA} (−54 mV), observed in basket cells one week after experimental status

epilepticus (Yu *et al.*, 2013), enhances average FS-BC frequency by over 30 Hz to the 80-250 Hz range associated with epileptic networks and degrades global network coherence. Although the depolarizing shift in E_{GABA} abolishes global network coherence, it supports a modest local coherence and leads to FS-BC sub network activity that results in enhanced network frequency. Our simulations indicate that networks with the depolarizing E_{GABA}, identified in FS-BCs after status epilepticus (Yu *et al.*, 2013), can support focal high frequency activity. In networks with -54 mV E_{GABA} activated by dendritic synaptic inputs, increases in extrasynaptic GABA currents, observed in FS-BCs following experimental status epilepticus (Yu *et al.*, 2013), further enhance average FS-BC frequency (Figs. 6(d), 6(f), 7(a), and 7(b)). These findings indicate that experimentally identified, seizure-induced increases in basket cell tonic GABA currents and depolarization of GABA reversal potential may undermine physiological gamma oscillations and contribute to the pathological, focally coherent high frequency firing observed in human and animal epilepsy (Bragin *et al.*, 1999; Worrell *et al.*, 2004; Worrell *et al.*, 2008).

Motivation for use of biophysically based neuron models

Combinations of theoretical and experimental studies have provided convincing evidence that fast-spiking interneurons contribute to the generation of gamma frequency network oscillations. Recent studies have identified that intrinsic properties of the individual cells in a network can play a critical role in determining the spatiotemporal patterns of network activity (Tateno *et al.*, 2004; Tateno and Robinson, 2006; Wang, 2010; Borgers and Walker, 2013). Thus, intrinsic properties of FS-BCs that underlie gamma frequency oscillations are likely to impact the emergent activity patterns in homogeneous interconnected networks. There is also emerging appreciation that the use of biologically based models may overcome issues concerning empirical classification of neurons into distinct firing types for theoretical analyses (Skinner, 2013). The membrane excitability properties of the FS-BC model used in the current study, described by the firing frequency-current input relationship (*f-I* curve), closely matched the *f-I* curve of the biological dentate FS-BCs (Fig. 1(c)) and thus simulated the active characteristics of the specific neuronal type under investigation. Additionally, most existing studies adopt model interneurons with high frequency firing in which intrinsic conductances and current injections are scaled to membrane surface area (Bartos *et al.*, 2002; Vida *et al.*, 2006; Kochubey *et al.*, 2011; Song *et al.*, 2011). Introducing experimentally derived synaptic, extrasynaptic or gap junctional conductances directly into model neurons where the intrinsic conductances are scaled to surface area could contribute to inaccuracies in estimation of the impact of the conductances under investigation. Indeed, our recent study found that the biphasic firing response generated by introducing depolarizing extrasynaptic GABA conductance in generic interneuronal models (Song *et al.*, 2011) was observed only when extremely high levels of extrasynaptic GABA conductance was introduced in biophysically based model FS-BCs (Yu *et al.*, 2013). Despite the limitation that the FS-BC model used in this study does not simulate the recently proposed sodium channel distribution in basket cell dendrites (Hu *et al.*, 2010), it includes dendritic potassium channels (see Methods) and reliably simulates the low R_{in} and *f-I* characteristics of biological dentate FS-BCs. While more detailed, morphologically realistic dentate FS-BC models are available (Norenberg *et al.*, 2010), these highly complex multi-compartmental models developed to examine purely passive properties are not the optimal choice for simulating network activity. Since, our goal was to study how network activity patterns are altered by introducing experimentally based levels of $g_{GABA\text{-}extra}$, the biophysically based, multi-compartmental active dentate FS-BC model was optimally suited for the current study.

Our simulations demonstrate that FS-BCs networks connected with fast GABA synapses with realistic synaptic parameters and connectivity show coherent firing in the gamma frequency range and confirm the findings of earlier studies using generic models of fast-spiking neurons (Bartos *et al.*, 2002). However, we find that gap junctional conductances have a rather modest effect on firing coherence in networks of biophysically based model FS-BCs activated by dendritic synaptic inputs. We propose that the combination of natural FS-BC input resistance and dendritic location of the coupling in our multi-compartmental model neurons provides a more faithful representation of biology. Dendritic gap junctions are known to modulate network dynamics in the presence of active dendrites (Saraga *et al.*, 2006). However, even though the FS-BC model incorporated active conductances, including calcium and potassium channels in all dendritic compartments, the restriction of sodium conductance to the somatic and proximal (1°) dendritic compartment may have contributed to the limited effect of gap junctional conductances on network activity. Interestingly, despite the caveat that our model FS-BCs did not replicate the gamma frequency intrinsic resonance (unpublished observations) of hippocampal fast spiking interneurons (Pike *et al.*, 2000), FS-BC networks with fast GABA synapses and anatomically realistic connectivity patterns developed robust synchrony in the gamma frequency range. Although the heterogeneity in current injections used in the current study were lower than those adopted in earlier studies using generic interneuronal models (Bartos *et al.*, 2002; Vida *et al.*, 2006), the current injections used in our study resulted in 10%–180% variability in FS-BC firing. Moreover, even when we replaced somatic current injections with biologically motivated asynchronous dendritic synaptic inputs at 200 Hz to activate FS-BCs, network activity consistently synchronized in the gamma frequency range. These results are consistent with recent simulation studies demonstrating that excitatory synaptic drive at frequencies between 20 and 200 Hz result in gamma oscillations in networks of fast-spiking interneurons (Kochubey *et al.*, 2011). Thus, the biologically based FS-BC network model developed here provides an ideal platform for future studies to examine how experimentally identified changes in dentate FS-BC active and passive conductances may impact the ability of FS-BC networks to sustain gamma oscillations.

Modulation of gamma frequency oscillations by extrasynaptic inhibition

Tonic GABA currents mediated by peri- and extrasynaptic GABA receptors are present in various interneuronal types including FS-BCs (Semyanov *et al.*, 2003; Glykys *et al.*, 2007; Krook-Magnuson *et al.*, 2008; Olah *et al.*, 2009; Mann and Mody, 2010; Yu *et al.*, 2013). Extrasynaptic GABA receptors contribute to the baseline levels of noise and influence neuronal excitability and gain (Mitchell and Silver, 2003; Farrant and Nusser, 2005). Additionally, experimental studies have demonstrated that rodents lacking GABA receptor subtypes that underlie tonic GABA currents show changes in gamma frequency oscillations (Towers *et al.*, 2004; Mann and Mody, 2010). It is known that both stochastic noise and synaptic parameters modulate network oscillations (Bartos *et al.*, 2007; Stacey *et al.*, 2009). In addition to their contribution to baseline noise, extrasynaptic GABA receptors contribute to the decay of synaptic receptors and slow spillover GABA conductances (Rossi *et al.*, 2003; Mtchedlishvili and Kapur, 2006; Santhakumar *et al.*, 2006; Glykys and Mody, 2007). Indeed, the decay of inhibitory synaptic kinetics in FS-BCs is modulated by 4,5,6,7-tetrahydroisoxazolo[5,4-c] pyridin-3-ol (unpublished observations), an agonist selective for $GABA_AR\ \delta$ subunits which mediate tonic GABA currents in FS-BCs (Yu *et al.*, 2013). Our simulations showing that increases in spillover GABA conductances decrease the frequency and coherence of gamma frequency oscillations (Figs. 4–7) are consistent with the reduction in network frequency and coherence when synaptic decay kinetics are prolonged (Brunel and Wang, 2003; Bartos *et al.*, 2007). However, in light of our conservative assumption of low spillover conductance in the pS range, it is possible that our simulations underestimate the magnitude of the effect of $g_{GABA\text{-}extra}$ on the frequency and coherence of network oscillations. Moreover, robust increases in synaptic inhibition during physiological and pathological neuronal activity are likely to be accompanied by enhancement of spillover GABA conductance which could further augment the impact of $g_{GABA\text{-}extra}$ on network oscillations. Our observation that systematic increases in the baseline $g_{GABA\text{-}extra}$ fail to modulate network oscillations in the absence of spillover conductance underscores the importance of synaptic kinetics in determining network oscillations. However, our simulation of baseline extrasynaptic GABA conductance as a deterministic leak conductance rather than stochastic noisy conductance precludes changes in baseline root-mean-square noise associated with increasing $g_{GABA\text{-}extra}$. Consequently, use of a deterministic leak conductance to simulate baseline tonic GABA conductance may have resulted in further underestimation of the impact of these conductances on network coherence.

The ability of $g_{GABA\text{-}extra}$ to modulate gamma oscillations can have considerable impact on the physiological and pharmacological modulation of gamma oscillations. Tonic GABA currents in FS-BCs are mediated by $GABA_ARs$ containing δ subunits (Yu *et al.*, 2013). $GABA_ARs\ \delta$ subunits are subject to modulation by several neuroactive compounds such as alcohol, neurosteroids and certain anesthetics (Stell *et al.*, 2003; Mody *et al.*, 2007; Brickley and Mody, 2012). Therefore, it is possible that certain neuroactive compounds act, in part, by modulating network oscillations as a consequence of their effect on $g_{GABA\text{-}extra}$. Moreover, recent findings that tonic GABA currents mediated by δ subunit containing $GABA_ARs$ are modulated by $GABA_B$ receptor activation (Connelly *et al.*, 2013; Tao *et al.*, 2013) suggest that physiological modulation of tonic GABA currents could regulate the robustness of network oscillations. Overall, our results demonstrating that FS-BC $g_{GABA\text{-}extra}$, especially spillover GABA conductance, reduces the frequency and coherence of network oscillations suggest that gamma oscillations may be regulated by physiological and pathological modulation of basket cell tonic inhibition.

Basket cell inhibitory plasticity impacts network oscillations: Implications for seizure disorders

Since our simulations showed that extrasynaptic GABA conductances modulate network oscillations, we further investigated the effect of seizure-induced depolarization of FS-BC GABA reversal potential, together with increase in extrasynaptic GABA conductance (Yu *et al.*, 2013), on network activity. In contrast to the absence of changes in network excitability (Yu *et al.*, 2013), simultaneous introduction of tonic GABA currents and depolarized GABA reversal resulted in a striking enhancement of network frequency and decrease in global coherence of FS-BC oscillations. The increase in network frequency and decrease in coherence in the presence of depolarizing shift in E_{GABA} and increasing $g_{GABA\text{-}extra}$ was evident at all levels of somatic excitatory current drive tested. This suggests that despite potential seizure-induced decreases in FS-BC excitatory drive (Zhang and Buckmaster, 2009), the depolarizing shift in E_{GABA} and increasing $g_{GABA\text{-}extra}$ in FS-BCs after status epilepticus could lead to increase in network frequency and reduce network coherence. The shift in E_{GABA} of synaptic and extrasynaptic GABA currents resulted in over 30 Hz increase in FS-BC firing (Figs. 4–7) and contributed to locally coherent network firing in the 80-250 frequency range observed in epileptic foci (Bragin *et al.*, 1999; Worrell *et al.*, 2004; Worrell *et al.*, 2008). Moreover, in networks activated by dendritic synaptic inputs, systematically increasing extrasynaptic GABA conductance further enhanced average FS-BC frequency when E_{GABA} is depolarizing. However, as noted earlier, the effect of increasing extrasynaptic GABA conductance on network frequency was variable between networks, possibly due to variability in synaptic input patterns. It is possible that the pathologically depolarized inhibitory synaptic drive resulted in a net, depolarizing synaptic input frequency, *albeit* sub threshold, greater than the 200 Hz of the dendritic synaptic input frequency. Thus, the reduction in synchrony observed in interneuronal networks activated by dendritic synaptic inputs with frequencies over 200 Hz (Kochubey *et al.*, 2011) could contribute mechanistically to the reduction in coherence observed in our networks simulated with depolarizing E_{GABA}. Simultaneously, it is notable that the coherence of physiological gamma oscillations is reduced upon implementing experimentally observed seizure-induced changes in

FS-BC tonic GABA currents and GABA reversal potential and could contribute to the memory deficits associated with epilepsy (Chauviere *et al.*, 2009; Narayanan *et al.*, 2012; Rattka *et al.*, 2013).

Taken together, our results demonstrate that homogeneous networks of biophysically based fast-spiking basket cells connected by fast GABA synapses develop robust synchrony in the gamma frequency range that are subject to modulation by extrasynaptic GABA conductances and changes in GABA reversal potential. The findings suggest that physiological and pharmacological enhancement of basket cell tonic inhibition and experimentally identified changes FS-BC GABA currents following status epilepticus can compromise gamma frequency oscillations and promote pathological high frequency network activity.

ACKNOWLEDGMENTS

This work was supported by NIH/NINDS NS069861 and NJCBIR 09.003-BIR1 to V.S. We thank Dr. Bala Chidambaram for discussions and technical assistance.

Author Contributions: A.P. performed all simulations; J.Y. performed physiological experiments; A.P. analyzed data; A.P. and V.S. interpreted results of experiments; A.P. and F.S.E. prepared figures; A.P. and V.S. authored the manuscript; A.P., J.Y., F.S.E., and V.S. edited and approved the manuscript. A.P. and V.S.: conceived and designed research.

Amitai, Y., Gibson, J. R., Beierlein, M., Patrick, S. L., Ho, A. M., Connors, B. W., and Golomb, D., "The spatial dimensions of electrically coupled networks of interneurons in the neocortex," J. Neurosci. **22**, 4142–4152 (2002).

Bartos, M., Vida, I., and Jonas, P., "Synaptic mechanisms of synchronized gamma oscillations in inhibitory interneuron networks," Nat. Rev. Neurosci. **8**, 45–56 (2007).

Bartos, M., Vida, I., Frotscher, M., Geiger, J. R., and Jonas, P., "Rapid signaling at inhibitory synapses in a dentate gyrus interneuron network," J. Neurosci. **21**, 2687–2698 (2001).

Bartos, M., Vida, I., Frotscher, M., Meyer, A., Monyer, H., Geiger, J. R., and Jonas, P., "Fast synaptic inhibition promotes synchronized gamma oscillations in hippocampal interneuron networks," Proc. Natl. Acad. Sci. USA **99**, 13222–13227 (2002).

Belluscio, M. A., Mizuseki, K., Schmidt, R., Kempter, R., and Buzsaki, G., "Cross-frequency phase-phase coupling between theta and gamma oscillations in the hippocampus," J. Neurosci. **32**, 423–435 (2012).

Bogaard, A., Parent, J., Zochowski, M., and Booth, V., "Interaction of cellular and network mechanisms in spatiotemporal pattern formation in neuronal networks," J. Neurosci. **29**, 1677–1687 (2009).

Borgers, C. and Walker, B., "Toggling between gamma-frequency activity and suppression of cell assemblies," Front. Comput. Neurosci. **7**, 33 (2013).

Bragin, A., Engel, J., Jr., Wilson, C. L., Fried, I., and Mathern, G. W., "Hippocampal and entorhinal cortex high-frequency oscillations (100–500 Hz) in human epileptic brain and in kainic acid–treated rats with chronic seizures," Epilepsia **40**, 127–137 (1999).

Bragin, A., Wilson, C. L., Almajano, J., Mody, I., and Engel, J., Jr., "High-frequency oscillations after status epilepticus: Epileptogenesis and seizure genesis," Epilepsia **45**, 1017–1023 (2004).

Bragin, A., Azizyan, A., Almajano, J., Wilson, C. L., and Engel, J., Jr., "Analysis of chronic seizure onsets after intrahippocampal kainic acid injection in freely moving rats," Epilepsia **46**, 1592–1598 (2005).

Bragin, A., Jando, G., Nadasdy, Z., Hetke, J., Wise, K., and Buzsaki, G., "Gamma (40–100 Hz) oscillation in the hippocampus of the behaving rat," J. Neurosci. **15**, 47–60 (1995).

Brickley, S. G. and Mody, I., "Extrasynaptic GABA(A) receptors: Their function in the CNS and implications for disease," Neuron **73**, 23–34 (2012).

Brunel, N. and Wang, X. J., "What determines the frequency of fast network oscillations with irregular neural discharges? I. Synaptic dynamics and excitation-inhibition balance," J. Neurophysiol. **90**, 415–430 (2003).

Buzsaki, G. and Draguhn, A., "Neuronal oscillations in cortical networks," Sci. **304**, 1926–1929 (2004).

Buzsaki, G. and Wang, X. J., "Mechanisms of gamma oscillations," Annu. Rev. Neurosci. **35**, 203–225 (2012).

Buzsaki, G., Buhl, D. L., Harris, K. D., Csicsvari, J., Czeh, B., and Morozov, A., "Hippocampal network patterns of activity in the mouse," Neuroscience **116**, 201–211 (2003).

Chauviere, L., Rafrafi, N., Thinus–Blanc, C., Bartolomei, F., Esclapez, M., and Bernard, C., "Early deficits in spatial memory and theta rhythm in experimental temporal lobe epilepsy," J. Neurosci. **29**, 5402–5410 (2009).

Colgin, L. L. and Moser, E. I., "Gamma oscillations in the hippocampus," Physiology **25**, 319–329 (2010).

Colgin, L. L., Denninger, T., Fyhn, M., Hafting, T., Bonnevie, T., Jensen, O., Moser, M. B., and Moser, E. I., "Frequency of gamma oscillations routes flow of information in the hippocampus," Nature **462**, 353–357 (2009).

Connelly, W. M., Fyson, S. J., Errington, A. C., McCafferty, C. P., Cope, D. W., Di Giovanni, G., and Crunelli, V., "GABAB receptors regulate extrasynaptic GABAA receptors," J. Neurosci. **33**, 3780–3785 (2013).

Csicsvari, J., Jamieson, B., Wise, K. D., and Buzsaki, G., "Mechanisms of gamma oscillations in the hippocampus of the behaving rat," Neuron **37**, 311–322 (2003).

Csicsvari, J., Hirase, H., Czurko, A., Mamiya, A., and Buzsaki, G., "Oscillatory coupling of hippocampal pyramidal cells and interneurons in the behaving Rat," J. Neurosci. **19**, 274–287 (1999).

Dyhrfjeld-Johnsen, J., Santhakumar, V., Morgan, R. J., Huerta, R., Tsimring, L., and Soltesz, I., "Topological determinants of epileptogenesis in large-scale structural and functional models of the dentate gyrus derived from experimental data," J. Neurophysiol. **97**, 1566–1587 (2007).

Engel, J., Jr., Bragin, A., Staba, R., and Mody, I., "High-frequency oscillations: what is normal and what is not?," Epilepsia **50**, 598–604 (2009).

Farrant, M. and Nusser, Z., "Variations on an inhibitory theme: Phasic and tonic activation of GABA(A) receptors," Nat. Rev. Neurosci. **6**, 215–229 (2005).

Fell, J., Klaver, P., Lehnertz, K., Grunwald, T., Schaller, C., Elger, C. E., and Fernandez, G., "Human memory formation is accompanied by rhinal-hippocampal coupling and decoupling," Nat. Neurosci. **4**, 1259–1264 (2001).

Fisahn, A., Pike, F. G., Buhl, E. H., and Paulsen, O., "Cholinergic induction of network oscillations at 40 Hz in the hippocampus *in vitro*," Nature **394**, 186–189 (1998).

Fukuda, T. and Kosaka, T., "Gap junctions linking the dendritic network of GABAergic interneurons in the hippocampus," J. Neurosci. **20**, 1519–1528 (2000).

Galarreta, M. and Hestrin, S., "Electrical and chemical synapses among parvalbumin fast-spiking GABAergic interneurons in adult mouse neocortex," Proc. Natl. Acad. Sci. USA **99**, 12438–12443 (2002).

Gibson, J. R., Beierlein, M., and Connors, B. W., "Functional properties of electrical synapses between inhibitory interneurons of neocortical layer 4," J. Neurophysiol. **93**, 467–480 (2005).

Glykys, J. and Mody, I., "The main source of ambient GABA responsible for tonic inhibition in the mouse hippocampus," J. Physiol. **582**, 1163–1178 (2007).

Glykys, J., Peng, Z., Chandra, D., Homanics, G. E., Houser, C. R., and Mody, I., "A new naturally occurring GABA(A) receptor subunit partnership with high sensitivity to ethanol," Nat. Neurosci. **10**, 40–48 (2007).

Gupta, A., Elgammal, F. S., Proddutur, A., Shah, S., and Santhakumar, V., "Decrease in tonic inhibition contributes to increase in dentate semilunar granule cell," J. Neurosci. **32**, 2523–2537 (2012).

Hefft, S. and Jonas, P., "Asynchronous GABA release generates long–lasting inhibition at a hippocampal interneuron-principal neuron synapse," Nat. Neurosci. **8**, 1319–1328 (2005).

Hines, M. L. and Carnevale, N. T., "The NEURON simulation environment," Neural Comput. **9**, 1179–1209 (1997).

Hirai, N., Uchida, S., Maehara, T., Okubo, Y., and Shimizu, H., "Enhanced gamma (30–150 Hz) frequency in the human medial temporal lobe," Neuroscience **90**, 1149–1155 (1999).

Hu, H., Martina, M., and Jonas, P., "Dendritic mechanisms underlying rapid synaptic activation of fast-spiking hippocampal interneurons," Science **327**, 52–58 (2010).

Jutras, M. J., Fries, P., and Buffalo, E. A., "Gamma-band synchronization in the macaque hippocampus and memory formation," J. Neurosci. **29**, 12521–12531 (2009).

Kochubey, S., Semyanov, A., and Savtchenko, L., "Network with shunting synapses as a non-linear frequency modulator," Neural Network **24**, 407–416 (2011).
Krook-Magnuson, E. I., Li, P., Paluszkiewicz, S. M., and Huntsman, M. M., "Tonically active inhibition selectively controls feedforward circuits in mouse barrel cortex," J. Neurophysiol. **100**, 932–944 (2008).
Lewis, D. A., Curley, A. A., Glausier, J. R., and Volk, D. W., "Cortical parvalbumin interneurons and cognitive dysfunction in schizophrenia," Trends Neurosci. **35**, 57–67 (2012).
Lisman, J. E. and Idiart, M. A., "Storage of 7 +/− 2 short-term memories in oscillatory subcycles," Science **267**, 1512–1515 (1995).
Mann, E. O. and Mody, I., "Control of hippocampal gamma oscillation frequency by tonic inhibition and excitation of interneurons," Nat. Neurosci. **13**, 205–212 (2010).
Mann, E. O., Suckling, J. M., Hajos, N., Greenfield, S. A., and Paulsen, O., "Perisomatic feedback inhibition underlies cholinergically induced fast network oscillations in the rat hippocampus *in vitro*," Neuron **45**, 105–117 (2005).
Mitchell, S. J. and Silver, R. A., "Shunting inhibition modulates neuronal gain during synaptic excitation," Neuron **38**, 433–445 (2003).
Mody, I., Glykys, J., and Wei, W., "A new meaning for "Gin & Tonic": Tonic inhibition as the target for ethanol action in the brain," Alcohol **41**, 145–153 (2007).
Montgomery, S. M. and Buzsaki, G., "Gamma oscillations dynamically couple hippocampal CA3 and CA1 regions during memory task performance," Proc. Natl. Acad. Sci. U.S.A. **104**, 14495–14500 (2007).
Morgan, R. J. and Soltesz, I., "Nonrandom connectivity of the epileptic dentate gyrus predicts a major role for neuronal hubs in seizures," Proc. Natl. Acad. Sci. U.S.A. **105**, 6179–6184 (2008).
Mtchedlishvili, Z. and Kapur, J., "High–affinity, slowly desensitizing GABAA receptors mediate tonic inhibition in hippocampal dentate granule cells," Mol. Pharmacol. **69**, 564–575 (2006).
Narayanan, J., Duncan, R., Greene, J., Leach, J. P., Razvi, S., McLean, J., and Evans, J. J., "Accelerated long-term forgetting in temporal lobe epilepsy: Verbal, nonverbal and autobiographical memory," Epilepsy Behav. **25**, 622–630 (2012).
Netoff, T. I., Clewley, R., Arno, S., Keck, T., and White, J. A., "Epilepsy in small-world networks," J. Neurosci. **24**, 8075–8083 (2004).
Norenberg, A., Hu, H., Vida, I., Bartos, M., and Jonas, P., "Distinct nonuniform cable properties optimize rapid and efficient activation of fast-spiking GABAergic interneurons," Proc. Natl. Acad. Sci. U.S.A. 107, 894–899 (2010).
Olah, S., Fule, M., Komlosi, G., Varga, C., Baldi, R., Barzo, P., and Tamas, G., "Regulation of cortical microcircuits by unitary GABA-mediated volume transmission," Nature **461**, 1278–1281 (2009).
Percha, B., Dzakpasu, R., Zochowski, M., and Parent, J., "Transition from local to global phase synchrony in small world neural network and its possible implications for epilepsy," Phys. Rev. E **72**, 031909 (2005).
Pike, F. G., Goddard, R. S., Suckling, J. M., Ganter, P., Kasthuri, N., and Paulsen, O., "Distinct frequency preferences of different types of rat hippocampal neurones in response to oscillatory input currents," J. Physiol. **529**(1), 205–213 (2000).
Rattka, M., Brandt, C., and Loscher, W., "The intrahippocampal kainate model of temporal lobe epilepsy revisited: Epileptogenesis, behavioral and cognitive alterations, pharmacological response, and hippoccampal damage in epileptic rats," Epilepsy Res. **103**, 135–152 (2013).
Rossi, D. J. and Hamann, M., "Spillover-mediated transmission at inhibitory synapses promoted by high affinity alpha6 subunit GABA(A) receptors and glomerular geometry," Neuron **20**, 783–795 (1998).
Rossi, D. J., Hamann, M., and Attwell, D., "Multiple modes of GABAergic inhibition of rat cerebellar granule cells," J. Physiol. **548**, 97–110 (2003).
Santhakumar, V., "Modeling mossy cell loss and mossy fiber sprouting in epilepsy," in *Computational Neuroscience in Epilepsy*, edited by Soltesz, I. and Staley, K. J. (Academic Press, 2008), pp. 89–111.
Santhakumar, V., Aradi, I., and Soltesz, I., "Role of mossy fiber sprouting and mossy cell loss in hyperexcitability: A network model of the dentate gyrus incorporating cell types and axonal topography," J. Neurophysiol. **93**, 437–453 (2005).
Santhakumar, V., Hanchar, H. J., Wallner, M., Olsen, R. W., and Otis, T. S., "Contributions of the GABAA receptor alpha6 subunit to phasic and tonic inhibition revealed by a naturally occurring polymorphism in the alpha6 gene," J. Neurosci. **26**, 3357–3364 (2006).
Saraga, F., Ng, L., and Skinner, F. K., "Distal gap junctions and active dendrites can tune network dynamics," J. Neurophysiol. **95**, 1669–1682 (2006).
Semyanov, A., Walker, M. C., and Kullmann, D. M., "GABA uptake regulates cortical excitability via cell type-specific tonic inhibition," Nat. Neurosci. **6**, 484–490 (2003).
Sik, A., Penttonen, M., and Buzsaki, G., "Interneurons in the hippocampal dentate gyrus: An *in vivo* intracellular study," Eur. J. Neurosci. **9**, 573–588 (1997).
Skinner, F. K., "Cellular-based modeling of oscillatory dynamics in brain networks," Curr. Opin. Neurobiol. **22**, 660–669 (2012).
Skinner, F. K., "Moving beyond type I and type II neuron types," F1000Research **2**, 1–7 (2013).
Song, I., Savtchenko, L., and Semyanov, A., "Tonic excitation or inhibition is set by GABA(A) conductance in hippocampal interneurons," Nat. Commun. **2**, 376 (2011).
Srinivas, M., Rozental, R., Kojima, T., Dermietzel, R., Mehler, M., Condorelli, D. F., Kessler, J. A., and Spray, D. C., "Functional properties of channels formed by the neuronal gap junction protein connexin36," J. Neurosci. **19**, 9848–9855 (1999).
Stacey, W. C., Lazarewicz, M. T., and Litt, B., "Synaptic noise and physiological coupling generate high-frequency oscillations in a hippocampal computational model," J. Neurophysiol. **102**, 2342–2357 (2009).
Stell, B. M., Brickley, S. G., Tang, C. Y., Farrant, M., and Mody, I., "Neuroactive steroids reduce neuronal excitability by selectively enhancing tonic inhibition mediated by delta subunit-containing GABAA receptors," Proc. Natl. Acad. Sci. U.S.A. **100**, 14439–14444 (2003).
Steriade, M., Contreras, D., Amzica, F., and Timofeev, I., "Synchronization of fast (30–40 Hz) spontaneous oscillations in intrathalamic and thalamocortical networks," J. Neurosci. **16**, 2788–2808 (1996).
Tao, W., Higgs, M. H., Spain, W. J., and Ransom, C. B., "Postsynaptic GABAB receptors enhance extrasynaptic GABAA Receptor function in dentate gyrus granule cells," J. Neurosci. **33**, 3738–3743 (2013).
Tateno, T. and Robinson, H. P., "Rate coding and spike-time variability in cortical neurons with two types of threshold dynamics," J. Neurophysiol. **95**, 2650–2663 (2006).
Tateno, T., Harsch, A., and Robinson, H. P., "Threshold firing frequency-current relationships of neurons in rat somatosensory cortex: Type 1 and type 2 dynamics," J. Neurophysiol. **92**, 2283–2294 (2004).
Towers, S. K., Gloveli, T., Traub, R. D., Driver, J. E., Engel, D., Fradley, R., Rosahl, T. W., Maubach, K., Buhl, E. H., and Whittington, M. A., "Alpha 5 subunit-containing GABAA receptors affect the dynamic range of mouse hippocampal kainate–induced gamma frequency oscillations *in vitro*," J. Physiol. **559**, 721–728 (2004).
Traub, R. D., Spruston, N., Soltesz, I., Konnerth, A., Whittington, M. A., and Jefferys, G. R., "Gamma-frequency oscillations: A neuronal population phenomenon, regulated by synaptic and intrinsic cellular processes, and inducing synaptic plasticity," Prog. Neurobiol. **55**, 563–575 (1998).
Uhlhaas, P. J. and Singer, W., "Abnormal neural oscillations and synchrony in schizophrenia," Nat. Rev. Neurosci. **11**, 100–113 (2010).
Vida, I., Bartos, M., and Jonas, P., "Shunting inhibition improves robustness of gamma oscillations in hippocampal interneuron networks by homogenizing firing rates," Neuron **49**, 107–117 (2006).
Wang, X. J., "Neurophysiological and computational principles of cortical rhythms in cognition," Physiol. Rev. **90**, 1195–1268 (2010).
Wang, X. J. and Buzsaki, G., "Gamma oscillation by synaptic inhibition in a hippocampal interneuronal network model," J. Neurosci. **16**, 6402–6413 (1996).
Wei, W., Zhang, N., Peng, Z., Houser, C. R., and Mody, I., "Perisynaptic localization of delta subunit-containing GABA(A) receptors and their activation by GABA spillover in the mouse dentate gyrus," J. Neurosci. **23**, 10650–10661 (2003).
White, J. A., Chow, C. C., Ritt, J., Soto-Trevino, C., and Kopell, N., "Synchronization and oscillatory dynamics in heterogeneous, mutually inhibited neurons," J. Comput. Neurosci. **5**, 5–16 (1998).
Whittington, M. A., Traub, R. D., and Jefferys, J. G., "Synchronized oscillations in interneuron networks driven by metabotropic glutamate receptor activation," Nature **373**, 612–615 (1995).
Whittington, M. A., Traub, R. D., Kopell, N., Ermentrout, B., and Buhl, E. H., "Inhibition-based rhythms: Experimental and mathematical observations on network dynamics," Int. J. Psychophysiol. **38**, 315–336 (2000).
Worrell, G. A., Parish, L., Cranstoun, S. D., Jonas, R., Baltuch, G., and Litt, B., "High-frequency oscillations and seizure generation in neocortical epilepsy," Brain **127**, 1496–1506 (2004).

Worrell, G. A., Gardner, A. B., Stead, S. M., Hu, S., Goerss, S., Cascino, G. J., Meyer, F. B., Marsh, R., and Litt, B., "High-frequency oscillations in human temporal lobe: Simultaneous microwire and clinical macroelectrode recordings," Brain **131**, 928–937 (2008).

Wulff, P., Ponomarenko, A. A., Bartos, M., Korotkova, T. M., Fuchs, E. C., Bahner, F., Both, M., Tort, A. B., Kopell, N. J., Wisden, W., and Monyer, H., "Hippocampal theta rhythm and its coupling with gamma oscillations require fast inhibition onto parvalbumin-positive interneurons," Proc. Natl. Acad. Sci. U.S.A. 106, 3561–3566 (2009).

Yu, J., Proddutur, A., Elgammal, F. S., Ito, T., and Santhakumar, V., "Status epilepticus enhances tonic GABA currents and depolarizes GABA reversal potential in dentate fast-spiking basket cells," J. Neurophysiol. **109**, 1746–1763 (2013).

Zhang, W. and Buckmaster, P. S., "Dysfunction of the dentate basket cell circuit in a rat model of temporal lobe epilepsy," J. Neurosci. **29**, 7846–7856 (2009).

See supplementary material at http://dx.doi.org/10.1063/1.4830138 for Supplementary Figures 1 and 2.